UNIVERSIDAD DE CHILE
FACULTAD DE CIENCIAS FÍSICAS Y MATEMÁTICAS
DEPARTAMENTO DE INGENIERIA DE MINAS

SCALE EFFECT ON THE POST-PEAK BEHAVIOR OF DACITE ROCK IN UNIAXIAL COMPRESSION TESTS

TESIS PARA OPTAR AL GRADO DE MAGISTER EN MINERÍA

MEMORIA PARA OPTAR AL TÍTULO DE INGENIERO CIVIL DE MINAS

CARLOS JAVIER ZUÑIGA NUÑEZ

PROFESOR GUÍA:
JAVIER VALLEJOS MASSA

PROFESOR CO-GUÍA:
KIMIE SUZUKI MORALES

MIEMBROS DE COMISIÓN
LUIS FELIPE ORELLANA ESPINOZA
JAVIER ARZUA TOURIÑO

SANTIAGO DE CHILE
2020

SCALE EFFECT ON THE POST-PEAK BEHAVIOR OF DACITE ROCK IN UNIAXIAL COMPRESSION TESTS

Actualmente los yacimientos minerales se están explotando a niveles cada vez más profundos, lo que significa que las operaciones mineras de hoy deben enfrentar los desafíos de los altos esfuerzos. En este contexto, la obtención de la curva completa de esfuerzo-deformación se ha vuelto crucial para comprender cómo se comporta la roca después de la ruptura.

En este trabajo se realizó una serie de pruebas de compresión uniaxiales para estudiar el efecto de escala en los comportamientos pre- y post-rotura en rocas tipo dacita de División el Teniente, CODELCO. Para las pruebas se utilizaron 30 muestras de roca dacita de tres tamaños de diámetros distintos: 50 mm, 98 mm y 143 mm.

A partir de las pruebas, se analiza el efecto del tamaño de la muestra sobre los parámetros mecánicos –parámetros elásticos, módulo de caída y resistencia residual– de la roca intacta. Resultados principales indican que la resistencia de esfuerzo máxima, el módulo de Young, los umbrales de cierre de microfracturas preexistentes, de iniciación de nuevas fracturas e interacción de fracturas, el módulo de caída y la relación de Poisson parecen ser independientes de la escala.

A partir del análisis del estudio, se ha introducido un nuevo parámetro de estudio, la resistencia residual diametral, que se refiere a la resistencia residual en la curva de deformación diametral-esfuerzo axial. Se concluye que este parámetro se ve afectado por el tamaño de la muestra y proporciona nueva información útil sobre el comportamiento de la roca posterior a la rotura.

ABSTRACT

Ore deposits are currently being exploited at ever deeper levels, which means that today's mining operations must face challenges associated to high-stress environments. In this context, to obtain the complete stress-strain curve is crucial for the understanding of post-peak behavior.

In this work, a series of uniaxial compression tests was carried out to study the effect of scale on pre- and post-peak behavior in dacite rocks from mine El Teniente, CODELCO. For the tests, 30 dacite rock samples of three different diameter sizes were used: 50 mm, 98 mm and 143 mm.

From the tests, the effect of the sample size on the mechanical parameters - elastic parameters, drop modulus and residual stress - of the intact rock is analyzed. Main results indicate that peak strength, Young's modulus, pre-existing microfracture closure thresholds, new fracture initiation and fracture interaction, drop modulus, and Poisson's ratio appear to be scale independent.

From the analysis of this work, a new study parameter has been introduced, the diametral residual stress, which refers to the residual stress in the diametral deformation-axial stress curve. It is concluded that this parameter is affected by the size of the sample and provides new useful information on the behavior of the rock after failure.

TABLE OF CONTENTS

TABLE OF CONTENTS

List of Figures

List of Tables

List of Appendix Figures

TABLE OF CONTENTS

List of Appendix Tables

1. Introduction

In the last century, the field of rock mechanics has extensively studied the behavior of specimens and rock masses before they break or collapse (Hawkes & Mellor 1970; Hoek & Brown 1980; Yoshinaka et al. 2008). However, what happens after failure has been considerably less studied due to the difficulty of estimating such effects. Moreover, mining designs are traditionally carried out with the aim of avoiding fracture, so knowing the behavior after failure was not considered necessary.

This has changed with the current mining conditions, mainly underground, which present high stresses due to the deepening of production levels and consequent high induced stresses. An improvement in rock qualities has also been observed with deepening production, but other factors, such as granulometry, hydraulic fracturing, the appearance of water, rock bursts, need to be better understood as the different conditions and effects on rock mass impact the design of tunnels, pillars, and equipment rooms. Similarly, the open-pit mining of today requires knowledge about fractured rock. This information is necessary for the stability of long-term slopes and landfill design, which uses already fractured rock.

To investigate the impact on rocks under different conditions, laboratory tests can be used to study the mechanical behavior of rock through compression tests. These are useful to generate a database that allows the changes to be quantified and analysed. Laboratory tests carried out in the last decades have established some standards that allow the comparison of results (Ulusay & Hudson 2007). Two of the main tests that have been used are simple compression and triaxial compression, which are generally performed to obtain pre-peak behavior (Hoek & Brown 1980). More expanded testing that considers post-fracture rock behavior would also be useful for mine design, risk analysis and numerical modeling.

In this study, a set of uniaxial compression tests is carried out obtaining of the complete stress-stain curve in dacite rocks of three sizes of different diameters, aims to determine and study the existence of the scale effect in the parameters obtained that define the behavior of the rock.

1.1. Preamble

Post-peak behavior has been considerably less studied than pre-peak, especially in rocks with brittle behavior due to the complexity of the laboratory procedure and the required equipment (Hudson et. Al. 1972; Ulusay & Hudson 2007). However, in recent years various studies have emerged focused on better understanding the characteristics and properties of post-peak behavior of various lithologies. These studies have been developed mainly through triaxial tests with considerably fewer uniaxial tests having been detailed in the literature, leaving a gap in the database and making it impossible to understand the complete progression of behavior in the different confinement conditions.

CHAPTER 1

In 2017, the Advanced Mining Technology Center (AMTC) in conjunction with the Department of Mining Engineering of the University of Chile, acquired a servo-assisted press with a capacity of 8,000 kN of compressive load. This equipment can perform testing with deformation control, obtaining records to evaluate the post-peak behavior of specimens for different sizes. Later in 2019, another servo-assisted press with a capacity of 3,000 kN was incorporated, which allows tests to be carried out on smaller specimens, mainly focused on a range between 30 mm and 100 mm in diameter. This equipment has allowed the complete stress-strain curve in a wide range of specimen diameters and lithological variety to be obtained through its current focus on uniaxial tests.

1.2. Motivation

Laboratory studies have made it possible to study various factors that influence the results and behavior of the rock, including rock dimensions (diameter and height), lithology, presence of discontinuities, temperature, strain rates, confining pressure, among others (Hawkes & Mellor 1970; Yoshinaka et al. 2008). The influence of these factors on post-peak behavior is not yet clear although recent studies have found approximations.

One of the most studied factors is the so-called scale effect, which refers to the change in the mechanical response of the rock as a function of volume. Hoek & Brown (1980) proposed a first approximation, which has been globally accepted. However, other authors (Masoumi et al. 2016) have proposed different approaches depending on the lithology and suggesting that the scale effect could be related to one or more rock influence factors, affecting each differently. Walton (2017), states that there are three main factors that generate the scale effect: the presence of discontinuities, the shape effect and the intact rock.

This work aims to determine the existence of this scale effect in dacite rocks for the parameters that define the post-peak behavior (drop modulus and residual stress) obtained through the obtain of complete stress-strain curves.

1.3. Objective of the Study

The general objective of this research is to study the scale effect of intact rock in post-peak behavior of dacite rock, through the performance of 30 uniaxial compression tests with complete stress-strain curve measurement in order to identify the main parameters that define the behavior.

1.4. Scope of the Study

a) Uniaxial compression tests on dacite specimens, from the El Teniente mine, Chile.

b) The samples selected to carry out the tests are free of discontinuities on their surface, so they are considered as intact rock.

c) Specimens with three different diameters: 50 mm, 98 mm and 143 mm and a height/diameter ratio of 2:1.

d) The 50 mm and 98 mm diameter specimens were carried out in a press with a maximum capacity of 3000 kN (MES300), while the 143 mm diameter specimens were carried out in a press with a maximum capacity of 8000 kN (MES800).

e) Measurement of axial and diametral strain using four linear variable differential transformers (LVDT) in conjunction with rosette strain gauges.

f) LVDT's were held with magnetic bases in the 98 mm and 143 mm diameter specimens while for the 50 mm tests an aluminum ring was used to hold the LVDT's around the specimens.

1.5. State of the Art

The main factor that influences post-peak behavior is the confining pressure to which the test is subjected, allowing the change from brittle to ductile behavior to be observed. Many studies, such as those by Walton (2017), Rochan (2017), Susheng (2019) or Meng (2015), allow us to observe this transition, demonstrating the important influence of confining pressure. Zhang & Li (2018), specifically studied the influence of confining pressure on post-peak behavior, performing tests on marble and granite with confining pressures of up to 120 MPa, demonstrating how behavior changes from a post-peak class II to a fully ductile class I (Figure 1.1).

On the other hand, the structures present in the samples and confining pressure can change the expected behavior of a sample. Arzua (2015) performed triaxial tests (1 MPa, 2 MPa, 4 MPa, 6 MPa, 10 MPa and 12 MPa of confinement) on granite specimens of 54 mm in diameter in order to measure the influence of artificial discontinuities on behavior, obtaining that the value of dilation angle depends of confining stress (it diminishes when confining stress increases).

Turichshev (2016) studied the effect of discontinuities with mineralogical fill in Andesite specimens with confining pressures between 2 and 60 MPa, concluding that the strength of the intact veined specimens and their behavior were controlled by mineral filled veins.

CHAPTER 1
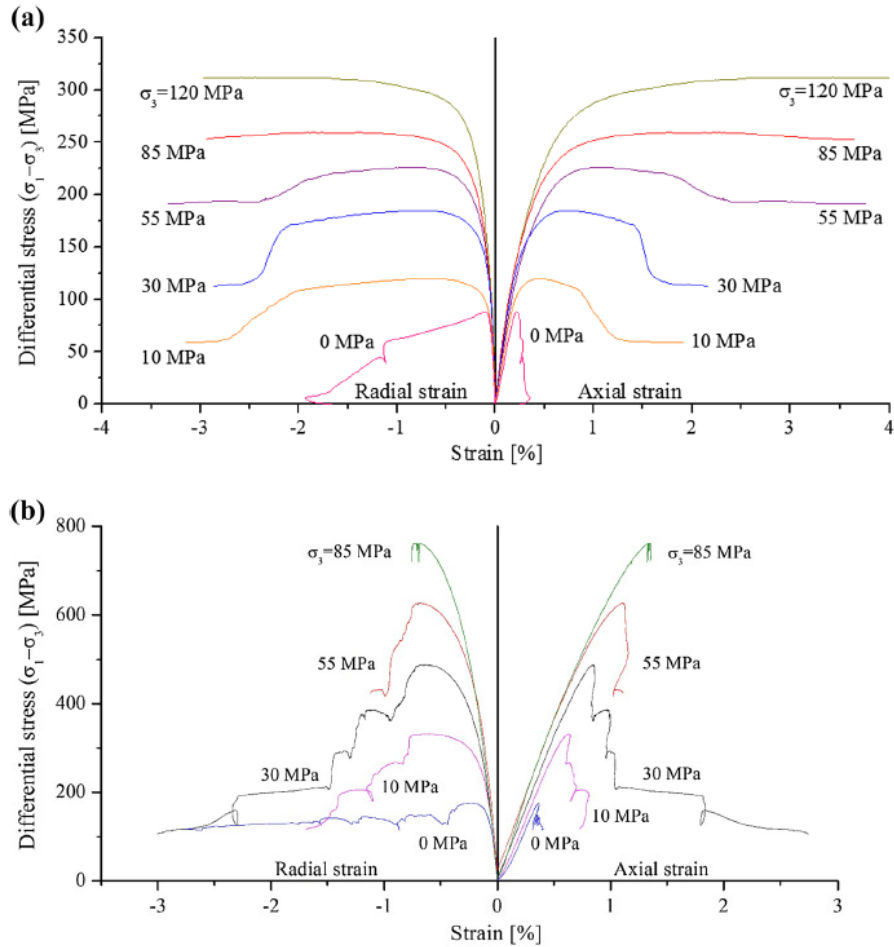
FIGURE 1.1 REPRESENTATIVE STRESS–STRAIN CURVES: (A) MARBLE SPECIMENS (B) GRANITE SPECIMENS (ZHANG & LI 2018)

Other authors have carried out studies that complement these works. Turichshev et al. (2014) carried out a series of triaxial tests on intact veined rock and successfully modelled the behavior through the Synthetic Rock Mass model. Munoz et al. (2016) presented a non-contact method for strain measurement applying three-dimensional digital image correlation (3D DIC), demonstrating that this method is better than conventional external strain measurement like strain gauges and LVDT. Taheri & Munoz (2019) studied the mechanism that controls violent/non-violent rock through an extensive experimental study using uniaxial and triaxial compression loading. Delonca & Vallejos (2020) developed a generalized failure criterion including the scale effect for predicting stress-induced overbreak around excavations using data from rock mass and intact rock scales.

As can be seen, most of the previous results have been for confining pressure tests. Few tests without confining pressure have been performed, with Akinbinu (2015) one of the few authors who has developed sets of uniaxial tests to obtain a complete stress-strain curve, obtaining that as the effect metamorphism increases, the state of stress, compaction of grains. Cementation and the brittleness of the rocks also increase.

CHAPTER 1

1.6. Previous Work

Although this study is a preliminary investigation, it is presented as a continuation of previous work carried out in the Rock Mechanics Laboratory of the Department of Mining Engineering of the University of Chile, done by the researcher Daniela Pollak Aguiló (Pollak & Vallejos 2018). That work summarized the considerations necessary to perform uniaxial compression tests with post-peak behavior measurement, in addition to some preliminary results of uniaxial tests, which were the first carried out with the MES800 press.

There are some considerations to take into account when performing uniaxial tests aimed to obtain post peak behavior measurements: stiffness of the equipment and servo-control, size of the specimen, strain rates and the characteristics of the press used. Table 1.1 compares the considerations suggested by the IRSM with those offered by the MES800 equipment demonstrating that the MES800 meets all the conditions for correct performance of post-peak behavior measurement.

TABLE 1.1: COMPARATIVE TABLE OF ISRM RECOMMENDATIONS AND PRESS MES800 (POLLAK ET AL. 2018)

Recommendation	ISRM	MES800 Press
High/diameter specimen ratio	2 to 3 References: HQ (63.5x158.8mm) 6" (147x367) 10" (254x508mm) 15" (381x762mm)	UCS up to 390mm diameter Triaxial up to 250 mm (In process)
Test speed	Force control: Speed of force application 0.5-1.0 MPa/s	This equipment allows speeds lower than 0.01 MPa/s
	Deformation control: axial and diametral for brittle behavior specimens: $1*10^{-3}$ mm/mm/s and $1*10^{-4}$ mm/mm/s, respectively	Preliminary tests were carried out during installation, using speeds of $2*10^{-9}$ mm/mm/s
Stiffness of equipment, k	>5 MN/mm	10.9 MN/mm
LVDTs precision	0.002mm in a range of 0.02mm 0.005mm in a range of 0.25mm	0.0004 mm

The main results of the study carried out by Pollak are summarized in Table 1.2, which shows the uniaxial tests carried out on the MES800 press with the calculation of the main parameters that define the pre- and post-peak behavior (Pollak et al. 2018). These results have been taken as the basis for implementing a new methodology to obtain the complete curve in uniaxial tests for rocks with post-peak class II behavior. Based on suggestions from the previous study, strain rates were modified to the lowest possible level (0.0001 mm/s) to obtain stable fracture propagation.

CHAPTER 1

Sample	Specimen size h/D (mm)	σ_c (MPa)	E (GPa)	ν	Speed test	σ_r (MPa)	M (GPa)
CX-107-(11)	318/142.8	118.4	39	0.42	3.57 kN/s (1)	N/A	N/A
CX-12	317.5/142.4	94.1	29.3	0.37	3.57 kN/s (1)	N/A	N/A
B-1	287/143	98.8	19.8	NIA	1.5 kN/s (1)	N/A	N/A
B-2	302/143	90.5	22.5	0.29	1.5 kN/s (1) / $3.3*10^{-5}$ mm/s (2)	61	38,5
DV-4	300.8/142.7	92.6	43.7	0.34	5 kN/s (1) / $3.3*10^{-5}$ mm/s (2)	62	48,3

h = Height; D = Diameter; σ_c = Uniaxial Compressive Strength; E = Young's Modulus

ν = Poisson's Ratio; σ_r = Residual Strength; M = Drop Modulus; N/A: Not applicable

(1) Force control; (2) Deformation control; NIA: No information available

A summary of uniaxial tests with post-peak behavior measurement performed by various authors and for various lithologies is presented in Figure 1.2 (Pollak et al. 2018). The summary shows that tests had only been carried out on specimens with smaller diameters (25-56 mm). Pollak (2018) was one of the first authors to expand the range of diameters, conducting tests on 143 mm diameter specimens. The aims of this current study are not only to increase the number of tests available for diameters of 50 mm and 143 mm, but also to incorporate an intermediate diameter of 98 mm that broadens the range of diameters on which data is available.

CHAPTER 1
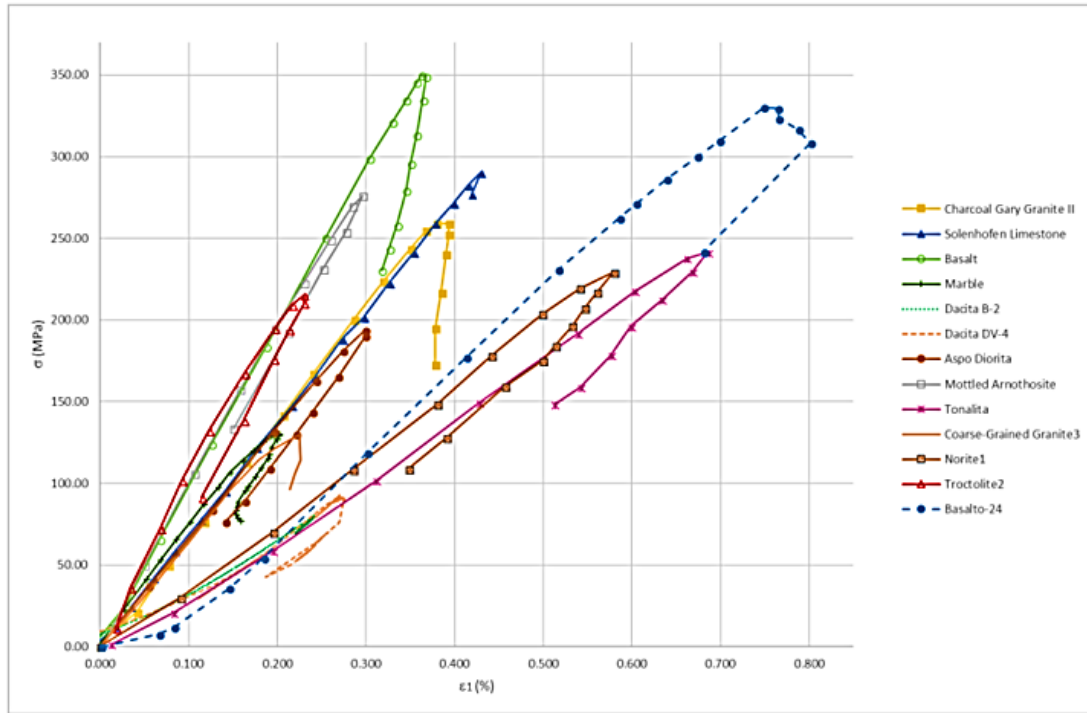
Lithology	Diameter	H/D	σ_c (MPa)	σ_{c50} (MPa)	E (GPa)	ν	M (GPa)
Charcoal Gary Granite II	25.4 or 50.8	2	259.0	259.7	70.0	--	374.2
Basalt	25.4 or 50.8	2	250.0	351.0	96.0	--	193.3
Solenhofen Limestone	25.4 or 50.8	2	290.0	290.8	129.0	--	129.0
Troctolite2	56	1.88	215.7	220.1	109.2	0.28	111.3
Norite 1	56	1.88	220.2	224.7	91.0	0.30	106.6
Mottled Anorthosite	56	1.88	276.3	282.0	96.8	0.32	97.0
Marble	50	2	130.6	130.6	69.8	--	94.7
Aspo Diorite	--	--	193.9	--	66.9	--	78.4
Granite 3	56	1.88	129.6	132.3	62.8	0.34	74.5
Basalto-24	47.5	2 to 2.4	330.0	327.0	49.5	--	55.3
Tonalite	56	1.88	241.4	246.4	38.1	--	51.4
Dacite CV-4	142.7	2.11	92.6	111.8	43.7	0.34	48.3
Dacite B-2	143	2.11	90.5	109.3	22.5	0.29	38.5

FIGURE 1.2: POST-PEAK DROP MODULUS (M) COMPARISON - CLASS II BEHAVIOR – WITH LVDT MEAUSUREMENT STRAIN (POLLAK ET AL. 2018)

1.7. Summary of the Study

The results of this study are presented in the following article:

"Scale effect on the post-peak behavior in uniaxial compression in dacite samples"

The results of this research were presented at MassMin 2020: Eighth International conference & Exhibition on Mass Mining.

Zuñiga, CJ, Vallejos, JA, Suzuki, K, Orellana, LF, Arzua, L 2020 'Scale effect on the post-peak behavior in uniaxial compression in dacite samples', MASSMIN 2020: Eighth International Conference & Exhibition on Mass Mining, Santiago, Chile, in press.

2. Scale effect on the post-peak behavior in uniaxial compression in dacite samples

2.1. Introduction

The exploitation of large mineral deposits in the world by open pit and underground mining often has a long life of mine, exceeding 100 years in some cases such as the El Teniente mine in Chile. These conditions typically cause changes in the geo-environmental conditions of operation during mine exploitation and are also associated with the evolution of the mining activity itself. Characteristic changes are related to the deepening of operations, directly impacting the induced stress and the response of the rock mass, the appearance of water, and other hazards.

To investigate the impact that these changes can produce, studies must be carried out under different scenarios. Laboratory tests are useful to generate a database to take into account for purposes of mining designs, risk analysis of mining operations, and/or numerical modeling. In the laboratory, it is possible to study the mechanical behavior of a rock through deformation tests at laboratory scale. Different types of laboratory tests have been widely carried out in the last decades for which some standards allow the comparison of results. Two of the main tests are simple compression and triaxial tests, which are generally performed to obtain pre-peak behavior (A in Figure 2.1).

Post-peak behavior, on the other hand, has been less studied, especially in rocks with brittle behavior due to the complexity of the laboratory procedure (Hudson et al. 1972; Ulusay & Hudson 2007). However, in recent years the number of studies has increased considerably, allowing a better understanding of the expected behavior for different types of rocks (Akinbinu 2015; Arzua 2015; Peng 2017). Laboratory tests have shown the brittle or ductile behavior of a rock specimen in a press (acting like a pillar in underground mines) depends on the relative stiffness between the specimen and the test frame (Ramírez-Oyanguren & Alejano 2008). A rock with brittle behavior fails violently and uncontrollably when it reaches its peak because there is an excess of elastic energy accumulated in the press that is suddenly released in the rupture and transformed into kinetic energy, projecting the fragments released from the specimen. At the peak, the stress that the rock can resist falls rapidly to zero (Rummel 1972). In the case of rocks with less stiffness than the test frame, violent failure is not generated, therefore the press needs to continue to add energy after the rupture so that the specimen continues to deform gradually.

Post-peak behavior in brittle rocks can show two distinct classes (Hudson et al. 1971): class I allows monotonic growth of axial strain until the sample fails. Class II requires reducing the stress or energy applied by the press on the sample much faster than class I to avoid sudden failure and take the characteristic path of its class (ABDE in Figure 2.1). In the laboratory, a rock sample that has behavior described by a class II stress-strain curve requires test equipment with greater stiffness than the sample, a servo control with fast response speed, and a strain rate that is very low. In addition, since the growth of axial strain is not monotonic, it is necessary to control the deformation rate of diametral strain (Ulusay & Hudson 2007). In other words, the equipment used for the test must be configured so that the applied stress responds to a constant diametrical strain

rate, decreasing the effort in case the measured strain rate increases with respect to the predicted strain rate or vice versa.

To the knowledge of the authors, few simple compression laboratory tests have shown in detail a complete stress-strain curve with post peak class II behavior. In general, these studies have not included a considerable number of tests on rocks with fragile behavior due to the low success rate that this test has had for the type of behavior mentioned. Consequently, a possible rock-mass scale approximation has not been studied in detail either. In this context, deepening this knowledge on a laboratory scale is especially relevant.
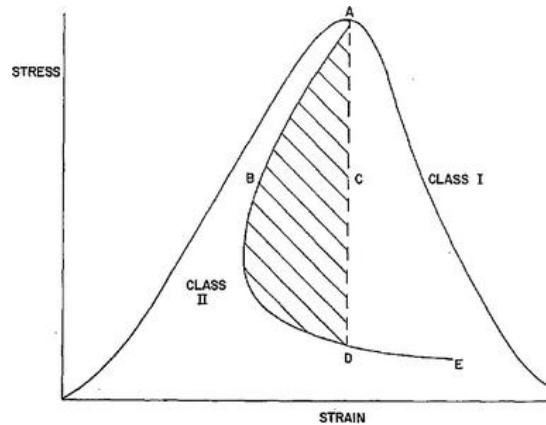

FIGURE 2.1: TYPES OF COMPLETE STRESS-STRAIN CURVES (HUDSON ET AL. 1971)

Stress-strain curves obtained from tests with and without confinement are useful to model the behavior of rock more realistically. For this, elastic models or elasto-plastic models can be used. Though elastic models are commonly used, they cannot represent the behavior of a rock under certain conditions, such as in areas of high fracturing where plastic deformations predominate. This prevents the different states of the rock mass from being represented. As an alternative, elasto-plastic models can be used, which do include plastic deformations and can also represent the post-peak behavior. Empirical or semi-empirical failure criteria are typically used, such as the Hoek and Brown or Mohr-Coulomb failure criteria. The constitutive model, Cohesion Weakening-Friction Strengthening (CWFS) (Hajiabdolmajid et al. 2002), describes the fragile failure process and is one of the most widely accepted models to realistically represent the different conditions that may exist within the rock mass (Walton 2019).

It is important to consider that the results of laboratory tests depend on the initial conditions of the samples. Some studies indicate that the sample size affects the pre-peak behavior (Hawkes & Mellor 1970; Hoek & Brown 1980; Yoshinaka et al. 2008). The size effect refers to the change in the mechanical response of the rock as a function of the volume, mainly due to three factors: the presence of discontinuities, the shape effect, and intact rock (Walton 2017). The last factor is related to test specimens without discontinuities and uniform grain size, which indicates that the grain size and the probability of generating a plane of weakness for a given size could partially explain the scale effect.

The scale effect of intact rock samples can be described by empirical relationships. A widely accepted relationship as the first approximation is the one proposed by Hoek & Brown (1980),

which indicates that the larger the diameter of the specimen, the lower the peak strength of the sample. This relationship is described in Equation (1), where $\sigma_{c,d}$ is the uniaxial compressive strength (UCS) for a specimen of diameter d, $\sigma_{c,50}$ is the UCS of a specimen of 50 mm diameter, and d is the diameter of the specimen in mm. Other authors (Masoumi et al. 2016) have proposed a model for intact rock characterized by having ascending and descending zones of peak resistance depending on the size of the samples. However, very few studies have been carried out to investigate these effects on post-peak behavior and have not obtained conclusive results on the analogy of these effects with pre-peak behavior (Walton 2017).

$$\sigma_{c,d} = \sigma_{c,50} \left(\frac{50}{d}\right)^{0.18}$$ (1)

This paper presents a preliminary study of the scale effect showing post-peak stress-strain curves in laboratory-scale dacite specimens subjected to uniaxial compression tests using a servo-controlled press. In particular, the drop modulus and residual stress are studied as the main parameters that define post-peak behavior. In addition, elastic parameters, damage thresholds, and peak strength are compared with previous studies.

To fulfill the objective of this work, the methodology that includes the preparation and sampling of the test specimens, the equipment used, and the laboratory procedure are first presented. Furthermore, the methodology used to calculate the pre- and post-peak parameters studied in this work is presented. Subsequently, the results of 21 tests on three different diameter sizes are presented and discussed. Finally, conclusions and suggestions are made for how future work could best extend our understanding of post-peak behavior of brittle rock.

2.2. Methodology

Uniaxial compression tests with stress measurement were performed with the aim of studying scale effects on pre- and post-peak parameters of dacite rock specimens from El Teniente mine, Codelco (Chile). This mine is characterized by having strong stockwork, even in small or local samples. The sector from which the samples were obtained is characterized by a considerable amount of rock bursts. Given this condition, previous laboratory tests without complete curve measurement on presses that are neither servo-controlled nor with sufficient stiffness to control the deformation test have resulted in violent failure modes causing multiple cracks. Typical values of the parameters that characterize this lithology are: Young's modulus of 30 GPa, Poisson's ratio of 0.2, and peak resistance between 109–130 MPa (De los Santos 2012).

The tests for this study were carried out on three different diameter sizes: 50 mm, 98 mm, and 143 mm. The height-diameter ratio is 2:1 for all samples according to the standard (Ulusay & Hudson 2007). Furthermore, the samples were prepared with a maximum deviation of parallelism between their basal faces of 0.001 rad and a flatness of the basal faces with a maximum difference of 0.01 mm. According to this same standard, it is recommended that at least five samples per size are tested, which is the minimum considered in this study.

Before carrying out the tests, a geological characterization was performed to select the samples that were considered as intact rock and had the most similarities. The main criteria for the selection of these samples were the following: 1) rock with no discontinuities visible on its surface and 2) relatively uniform grain size. This selection was made to isolate the influence of intact rock size

on the different parameters covered in this study. It should be noted that it is not possible to ensure that the selected samples do not have any discontinuities. Defects can be present at a microscale or with little persistence within the sample and invisible on the surface. The general aspects of selected samples showed that the rock was composed of a fundamentally homogeneous mass corresponding to 80% of the rock in which it is not possible to identify the grain size, while the other 20% was made up of phenocrystals. No considerable changes were observed on the surface of the rock, and its color was whitish-green. In addition, ten thin sections were prepared and selected from representative samples of each size to check the mineralogical composition at microscale. Results showed that the mineralogy of the tested rock consisted of four main elements: quartz (30%), plagioclase (35%), feldspars (15%), and biotite (20%).

The tests were carried out using two servo-assisted presses belonging to the Department of Mining Engineering of the University of Chile, which were acquired in conjunction with the Advanced Mining Technology Center (AMTC). Samples of d = 50 mm and d = 98 mm were tested in the MES300 press with a maximum capacity of 3,000 kN, and samples of d = 143 mm in the MES800 press with a maximum capacity of 8,000 kN (Figure 2.2). Both presses were used in this study due to their range of application, which allowed samples of different sizes to be tested. Both servo-assisted presses are controlled by the same PCD2K software (Servosis 2020) that controls the strain rates and acquires the test data.

FIGURE 2.2: SERVO-ASSISTED PRESSES USED TO PERFORM THE UNIAXIAL COMPRESSION TESTS: ON THE LEFT, MES300 PRESS WITH 3,000 KN CAPACITY, AND ON THE RIGHT, MES800 PRESS, WITH 8,000 KN CAPACITY

In addition, the same strain measurement instruments were used in both presses to reduce measurement errors when using different instruments. The strains are controlled using the PCD2K software through the conversion of the analog signal and measured in the samples through four Linear Variable Differential Transformers (LVDTs), two radial and two axial, and a strain gauge rosette located in the center of each specimen (Figure 2.3). The use of both measurement instruments allowed the identification of differences related to the measured strain and possible sources of errors.
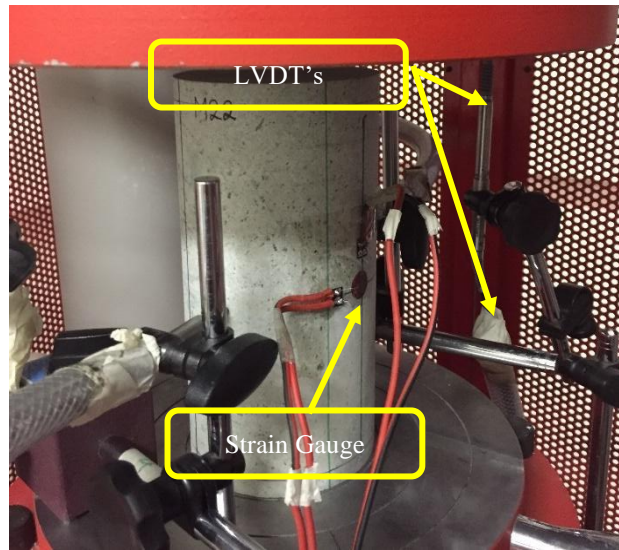
CHAPTER 2

FIGURE 2.3: TEST SET-UP ON A SPECIMEN OF D = 143 MM

Preliminary tests on dacite specimens resulted in brittle behavior and highly unstable fracture propagation, consistent with post-peak class II behavior. Based on this observation, during the test when the predicted peak strength approached, the specimens were controlled by adjusting the diametral strain (Ulusay & Hudson 2007).

The procedure used in the tests was as follows:

a) Test with force control (application of stress increased at a constant rate) up to 70% of the estimated UCS, which is approximately 109 MPa according to previous studies carried out by De los Santos (2012);
b) Then, switch to Diametral Strain Control to keep deformation rates constant;
c) Finally, upon entering the post-peak zone, double the diametral deformation rates to reduce the duration of the test.

Since the load or deformation rates must be the same for the different sizes, custom configurations were applied to each sample size as presented in Table 2.1.

TABLE 2.1: TEST CONFIGURATION BY SPECIMEN SIZE

Diameter Size (mm)	Force Control up to 70% of UCS (kN/min)	Pre-peak Diametral Strain Control (mm/min)	Post-peak Diametral Strain Control (mm/min)	Number of tests performed
50	5	0.0002	0.0004	10
98	10	0.0004	0.0008	10
143	15	0.0006	0.0012	10

CHAPTER 2

After the test, a record of the failure mode (Basu et al. 2013) of the sample was made through photographs and mapping of the surface, which provided a complete view of the surface, facilitating the recognition of the failure mode and persistence of the fractures generated.

The pre-peak elastic parameters were calculated according to the methodology proposed by Eberhardt (1998) after measuring strains and stresses:

    a) Young's modulus (E) is determined with the section of the axial stress-strain curve in which the slope of the curve is constant, a section that defines the linear elastic zone. This section is identified using the moving average slope along the entire curve, thus determining the part of constant slope (Figure 2.6 (a))

    b) The Poisson's ratio is determined as the ratio between the slopes of the axial stress-strain curve and the diametral stress-strain curve (Ulusay & Hudson 2007).

    c) The damage thresholds (Cai et al. 2004) are defined at the beginning of the linear elastic zone (σ_{cc}), when the crack volumetric strain begins to increase (σ_{ci}) and when the total volumetric strain slope becomes zero (σ_{cd}).

This methodology was replicated to estimate the drop modulus of the samples, which was defined as the post-peak section of the axial stress-strain curve slope that is constant and until the residual stress is reached. The residual stress is the stress value that remains constant even though the axial or diametral strain increases.

CHAPTER 2

2.3. Results

This section presents the complete stress-strain curves obtained in the tests successfully performed, and then the parameters estimated by the methodology previously presented.

Figure 2.4 shows six stress-strain curves obtained for the different diameters tested. In these tests, as in the rest of the samples, the curves exhibited post-peak class II behavior. The curves had a very similar general shape except for the resulting strain-stress magnitudes in each case.

The axial deformation rate was null or minimally variable in the final stages of the tests (over 0.25% of diametral deformation). In all tests, the axial deformation curves did not show residual stress because the type of rock tested allowed the samples to deform mainly along their diameter. In this way, the same level of axial deformations was constant while the diametral strain increased.

On the other hand, in the diametral strain curves, a residual stress was observed in most of the curves obtained. Some authors have obtained similar curves (Hudson 1971), although each author has focused on different parameters, such as the effect of rock metamorphism (Akinbinu 2015) or dilatation (Zhao & Cai 2010) for example. In general, the study parameters have historically been calculated on the stress-axial strain curves. This residual stress is related to the resistance capacity of the first macro crack that is generated during the test. It was observed that the diametral strain in the post-peak zone was largely defined by the shape and persistence of this first generated macro crack. One important observation made was that the crack generated continued to propagate or generate new cracks when reaching the residual stress, i.e. for the same stress level, the cracks can continue to propagate.

It is worth mentioning that the tests included in this investigation had no influence of discontinuities in their failure mode or in the kind of post-peak behavior obtained. Only a minimum number of samples had some discontinuity, and a very low percentage of these structures failed. The failure mode of all samples was by matrix, as expected due to the absence of structures.

A recurring trend observed was that as the diameter of the sample increased, the damage in the post-test samples increased in terms of the number of fractures and extent of cracks. Figure 2.5 shows that there were cracks slightly visible to the naked eye in the samples of d = 50 mm and multiple cracks in the samples of d = 143 mm. Smaller diameter samples showed intact basal faces in most cases after testing, maintaining much of the initial volume. In samples of d = 50 mm, axial fractures were observed by splitting and others by shear, according to the classification of failure modes (Basu et al. 2013). As the size of the samples increased, the cracks crossed the entire sample. In some cases, the samples were even divided into two or more parts. Possibly this was because the larger the size, the greater the amount of energy applied to the samples. Therefore, when this energy was released during the failure, it generated more damage.
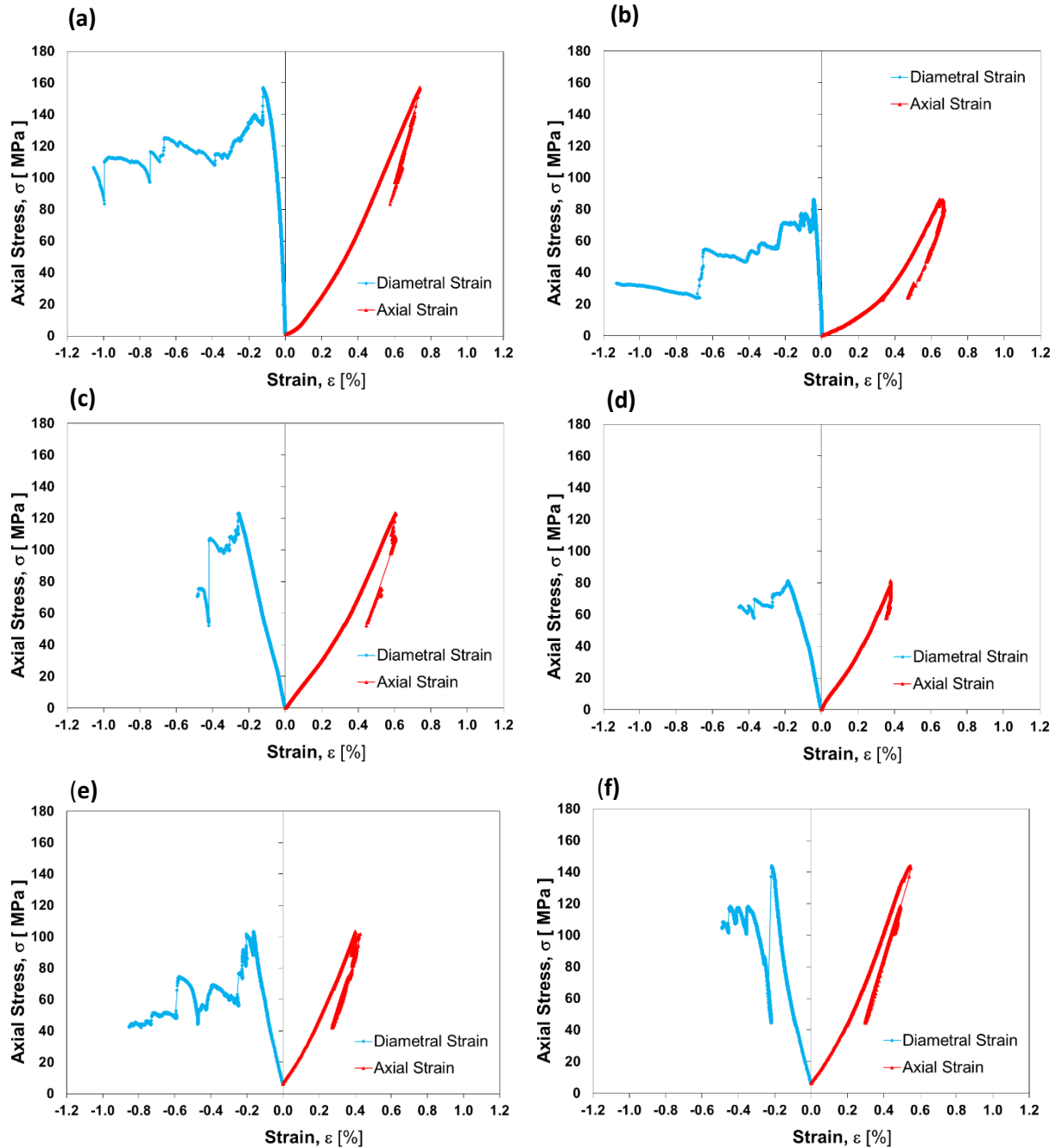
CHAPTER 2

(a)

(b)

(c)

(d)

(e)

(f)

FIGURE 2.4: STRESS-STRAIN CURVES MEASURED WITH LVDT'S FOR SAMPLES OF D = 50 MM (A AND B), D = 98 MM (C AND D), AND D = 143 MM (E AND F)

The calculation of elastic parameters was carried out according to the methodology proposed by Eberhardt et al. (1998), which allowed the sections of the curves in which these parameters should be calculated to be discriminated with greater certainty. Figure 2.6 shows an example of the calculation of these parameters for the test presented in Figure 2.4 (a). The change in the slope that defines the damage thresholds can be observed.

CHAPTER 2

(c) d=143 mm

(b) d=98 mm

(a) d=50 mm
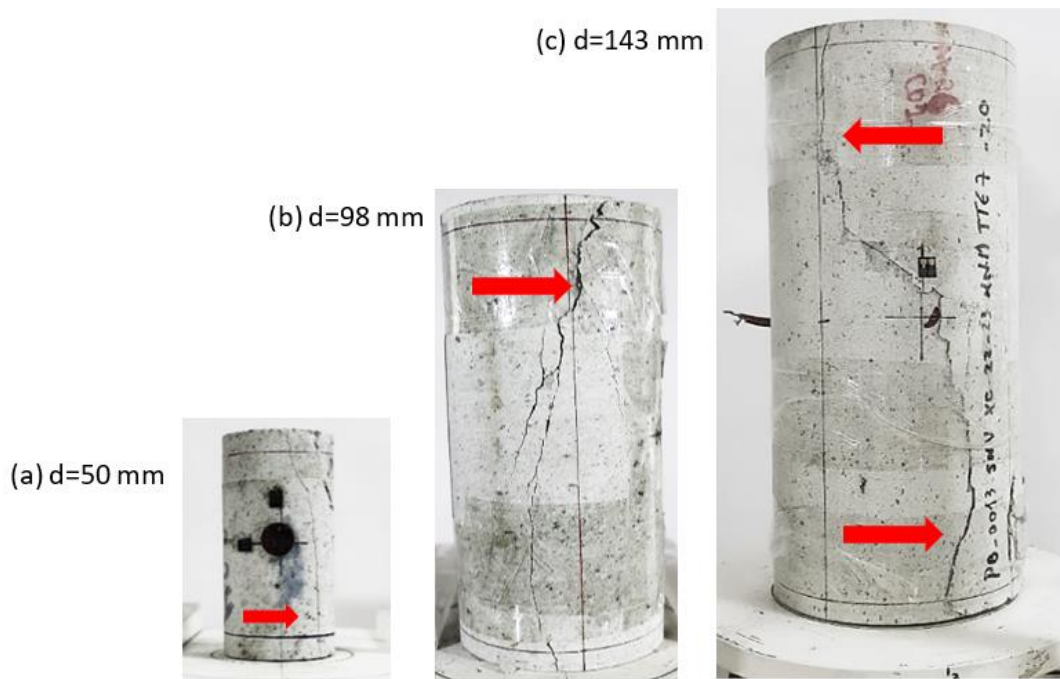
FIGURE 2.5: PHOTOGRAPHIC RECORD AFTER THE TEST FOR DIFFERENT DIAMETERS
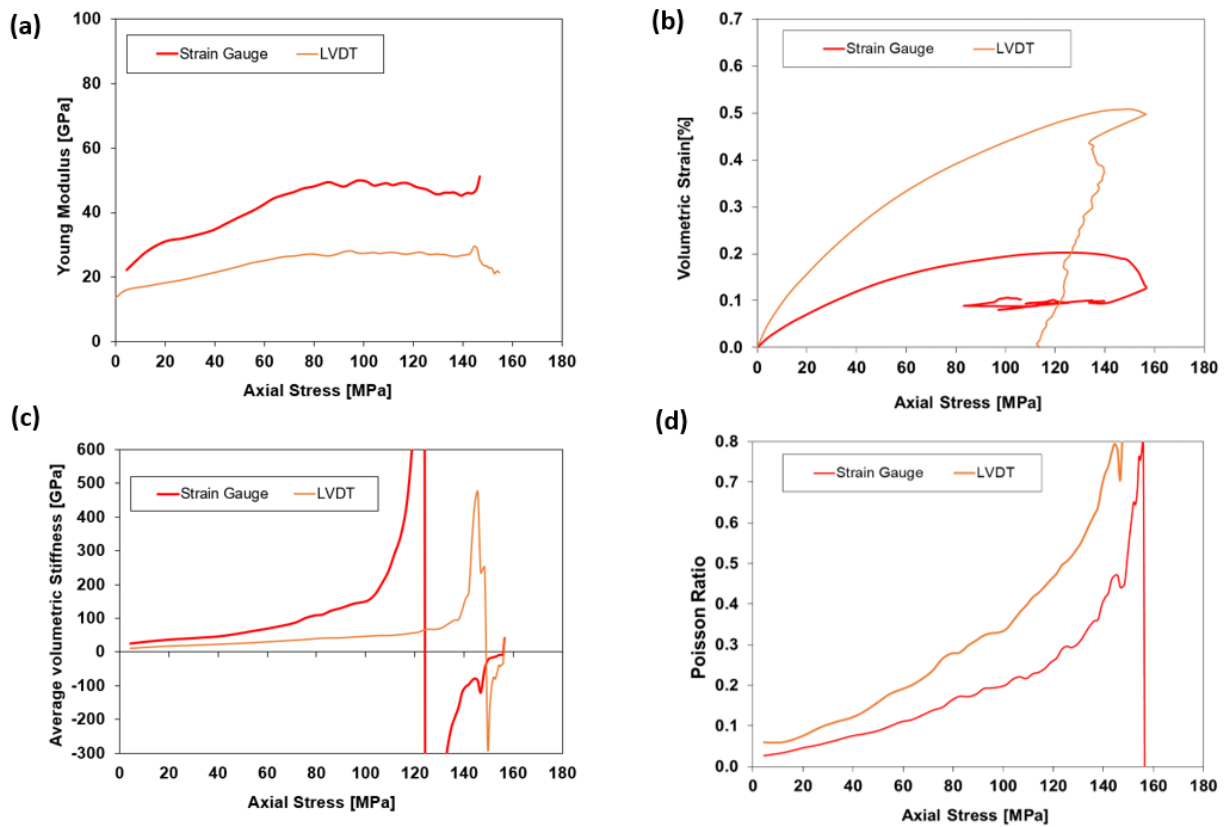
FIGURE 2.6: ESTIMATION OF PARAMETERS FOR SAMPLE M4A: (A) YOUNG'S MODULUS AND σ_{CC}, (B) σ_{CI}, (C) σ_{CD} AND (D) POISSON'S RATIO

Table 2.2 summarizes the parameters obtained for each size according to the methodology presented. As mentioned above, post-peak parameters, such as the drop modulus and the diametral residual stress were calculated analogously.

TABLE 2.2: SUMMARY OF RESULTS FOR EACH DIAMETER OF SAMPLE

Diameter of samples (mm)	Peak strength (MPa)	LVDT E (GPa)	LVDT Poisson's ratio	Strain Gauge E (GPa)	Strain Gauge Poisson's ratio	Drop modulus (GPa)	Residual stress (MPa)	Number of tests successfully performed
50	96.9	22.4	0.18	38.3	0.22	34.2	73.8	9
98	92.4	23.0	0.38	33.3	0.25	39.3	63.0	7
143	109.7	25.9	0.37	39.0	0.27	30.8	56.6	5

The damage thresholds found (σ_{cc}, σ_{ci} and σ_{cd}) presented a very small variation among samples of different sizes. On average, values of $\sigma_{cc} = 56$ MPa, $\sigma_{ci} = 72$ MPa and $\sigma_{cd} = 89$ MPa were obtained. Although these values are higher than the average of other rock lithologies (Cai et al. 2004), they are not significantly different from other studies that have been carried out in the same lithological complex (Turichshev & Hadjigeorgiou 2016).

2.4. Discussion

Class II post-peak behavior was obtained in all the samples tested. This behavior is not necessarily characteristic of the lithology tested or others with similar parameters, but rather depends mainly on the brittleness of the rock and the ability to sustain itself post failure (Akinbuku 2016). Previous studies using procedures that did not allow the definition of the complete curve have shown violent and multiple failure in dacite samples (De los Santos 2012).

Figure 2.7 shows a post-test sample of d = 143 mm controlled by a diametral strain rate of 0.001 mm/min. Multiple failures and the disintegration of the upper basal face can be observed, which contrasts with the sample tested in Figure 2.5 (c). Tested samples look different even though the speed used was only 33% higher. Results suggest that small changes in the test speed can generate a large increase in energy release that propagates multiple cracks, which is highly unstable when reaching the peak strength. This result justifies the low strain rates used in the tests.

FIGURE 2.7: SAMPLE OF D = 143 MM TESTED WITH DIAMETRAL STRAIN CONTROL AT 0.001 MM/MIN DIAMETRAL STRAIN RATE

This indicates that relatively low strain rates are required to achieve control of the test since this inherent brittleness of the matrix rock is what predominates in the rupture of the samples. Thus, the rates used in the tests have been empirically tested so that the propagation of the cracks at this rate is the least violent possible, allowing the press to react in time to control strains and avoid sudden failure. In a post-peak class II sample, a decrease in the axial strain was observed upon reaching the peak strength. Therefore, the press must generate a discharge of force at the peak to control the failure that occurs (Rummel 1972). In case of not doing so, an unstable propagation of the fault occurs, so that results like those in Figure 2.7 are obtained.

However, the samples are highly unstable for the failure that occurs at peak strength. It has been empirically proven that increasing the strain rates after that threshold does not prevent the propagation of this generated failure from being controlled. Therefore, the methodology proposes doubling the test speed rates once the test is in the post-peak stage, and in this way, the test time for these samples can be considerably reduced. Without duplicating the speeds, test time can exceed 24 hours. Using the methodology proposed here, the average test time for the samples was 10 hours.

One interesting observation is that as the diameter of the sample increased, the success rate of the tests was lower. A total of ten tests were performed for each diameter size (Table 2.1), of which nine were successful for the 50 mm diameter specimens, seven for the 98 m diameter specimens, and only five for the 143 mm diameter specimens. These results suggest that the strain rates that different sizes can support are not necessarily the same. This could be explained with the reasoning suggested by Hoek & Brown (1980) that by increasing the size of the specimens, it is more probable that there are defects inside the specimen that favor the propagation of fractures once the failure has started.

Table 2.2 shows that there are considerable differences in the parameters for the two strain measurement methods used. On the one hand, strain gauges are a local strain measurement method that is commonly used in laboratory tests. Previous studies indicate similar values to those obtained in this study with the measurement of the strain gauge. On the other hand, the deformation measurements obtained with the LVDTs may require some adjustment because these devices measure specimens globally (Alejano et al. 2018; 2020, Munoz et al. 2016), then, tilting or other external movements during the performance of the test may add strain through the mobile parts of the press or deform the sample geometry. It is important to note that the complete post-peak curve

CHAPTER 2

is only observed when measurements obtained from LVDT are used. An LVDT measurement includes elastic and plastic strains, which are produced by the cracks generated during the test.

Elastic parameters do not show a statistically relevant variation if different sizes are compared, as presented in Figure 2.8 (a) and (b). These results may be explained by the fact that the intact rock presents similar behavior in the different scales tested. Another possibility is that the presence of discontinuities influences the scale effect, which means that on a larger scale, a larger number of discontinuities increases the probability of failure at lower stress levels. In this study, no statistically relevant variations were observed possibly because the samples selected did not have discontinuities visible on their surfaces.

Post-peak parameters are estimated using deformations measured using LVDTs, as presented in Figure 2.8 (c) and (d). Strain gauges are not capable of measuring the deformations once the peak is reached for two reasons: (1) if the strain gauge lies just above the generated macro crack, then the strain gauge will break and stop measuring; (2) if the strain gauge is not above the macro crack, it will not record the localized strains precisely in those macro cracks. Results did not show scale dependency on the drop modulus (Figure 2.8 (c)), but there was an indication of a trend in the diametral residual stress (Figure 2.8 (d)).
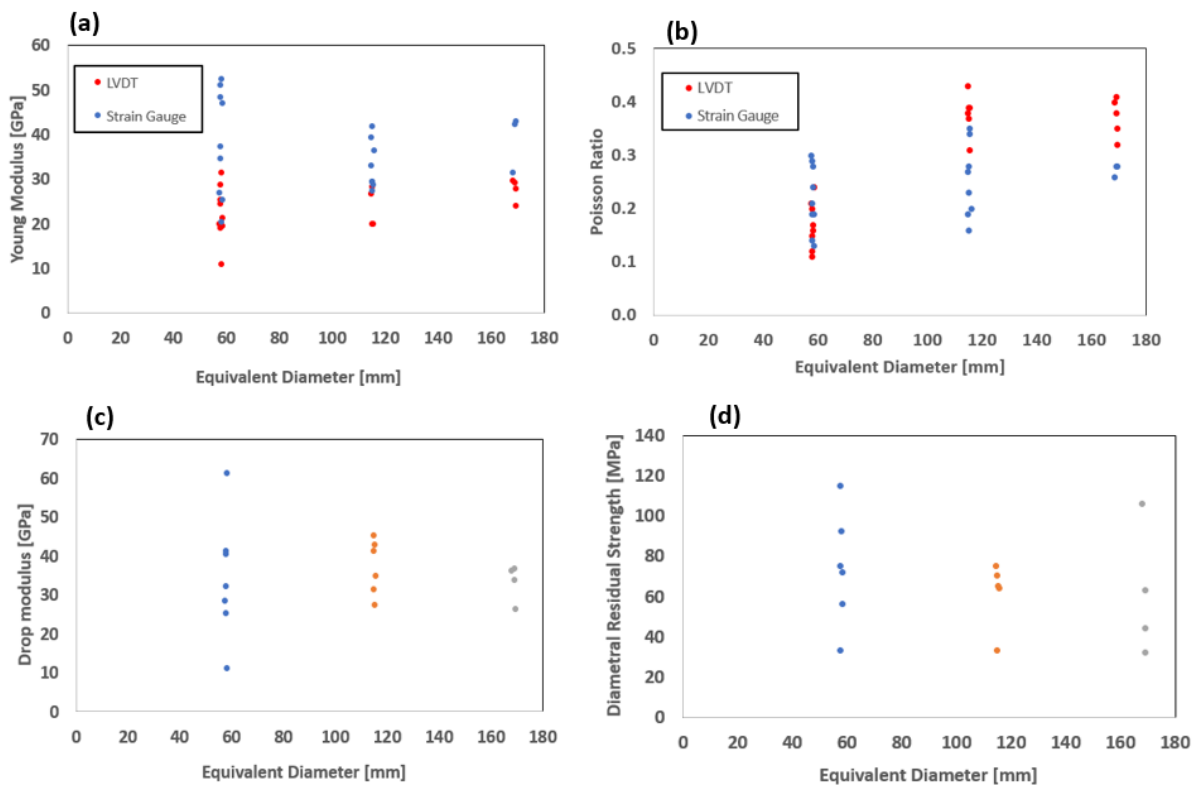
FIGURE 2.8: SUMMARY OF PARAMETERS OBTAINED AS FUNCTION OF SCALE: (A) YOUNG MODULUS (B) POISSON'S RATIO (C) DROP MODULUS, AND (D) DIAMETRAL RESIDUAL STRESS

Young's modulus slightly increased with the diameter when strain gauge measurements were compared, but the increase was not significant and is within the natural variability range of the rock. The same was observed for the Poisson's ratio. A considerable difference occurred in the measurements made using LVDT when samples of d = 50 mm and d = 98 mm were compared.

CHAPTER 2

This difference could be associated with a change in the method of strain measurement, in which the LVDTs were held with a magnetic base in the lower plate of the press for the 98 mm diameter specimens possibly producing some error of measurement of indirect strains. Regarding the post-peak parameters, there is an indication of a trend in the diametral residual stress, with a decrease of 22% from d = 50 mm to d = 143 mm. This trend would be expected to be maintained with more tests since it was observed that the samples with the largest diameter received greater damage after reaching the peak, which would indicate that the greater the damage, the less the stress that the specimen can withstand.

Figure 2.8 presents results with high variability at smaller sizes, which agree with the definition of the Representative Elementary Volume (REV) (Bear 1972). This variability reduces the possibility of finding a trend in the results because of the wide range of these results, especially in smaller sizes. A possible solution to this problem could be to increase the number of samples and the size of samples tested in order to reduce this variability and allow the existence of any trend related to the scale effect to be identified with greater certainty or prove that it is inherent to this rock type. However, increasing the size makes it difficult to obtain samples with no discontinuities, preventing the effect of intact rock from being evaluated. Furthermore, the REV would be impossible to achieve in laboratory tests based on the samples used to evaluate the parameters of a rock mass (Schultz 1995).

Peak strength does not show any scale-effect trend, contrary to that obtained by Hoek and Brown (1980). However, these results are not unexpected since, in other studies, similar behavior was obtained when isolating the effect of intact rock (Masoumi et al. 2016). The results show variability for each size, and this may be due to geological variability. However, although the samples come from the same sector and are visibly homogeneous, other factors such as internal defects or microstructures could affect peak strength. Figure 2.9 (a) shows the peak strength values (blue point) for three different sizes of the same initial piece of rock. These values of peak strength are similar to each other for the different diameters, which a priori justifies this variability with the reasons discussed. This could indicate that the existence of the scale effect is conditioned to other factors that influence peak strength and not to intact rock. These other factors could be the number of discontinuities present in the rock, the shape effect (height-diameter ratio), or the type of rock itself (brittle or ductile).

One of the main observations regarding the stress-strain curves (Figure 2.4) is the shape of the diametral strain curve. This curve is characterized by having pronounced breaks, and although the curves are not equal in magnitude for the different tests, they do maintain the same general shape. These differences in magnitude could be due to the deformation measurement system (LVDTs). However, although the magnitudes could contain measurement errors, the same general shape of the curve in all the tests suggests that the behavior is similar in all samples.

The damage thresholds do not present significant trends in relation to the scale of the samples tested; in this case, similar values are observed for the results obtained with both LVDTs and Strain Gauges (Figure 2.9 (b), (c) and (d)).

(a)

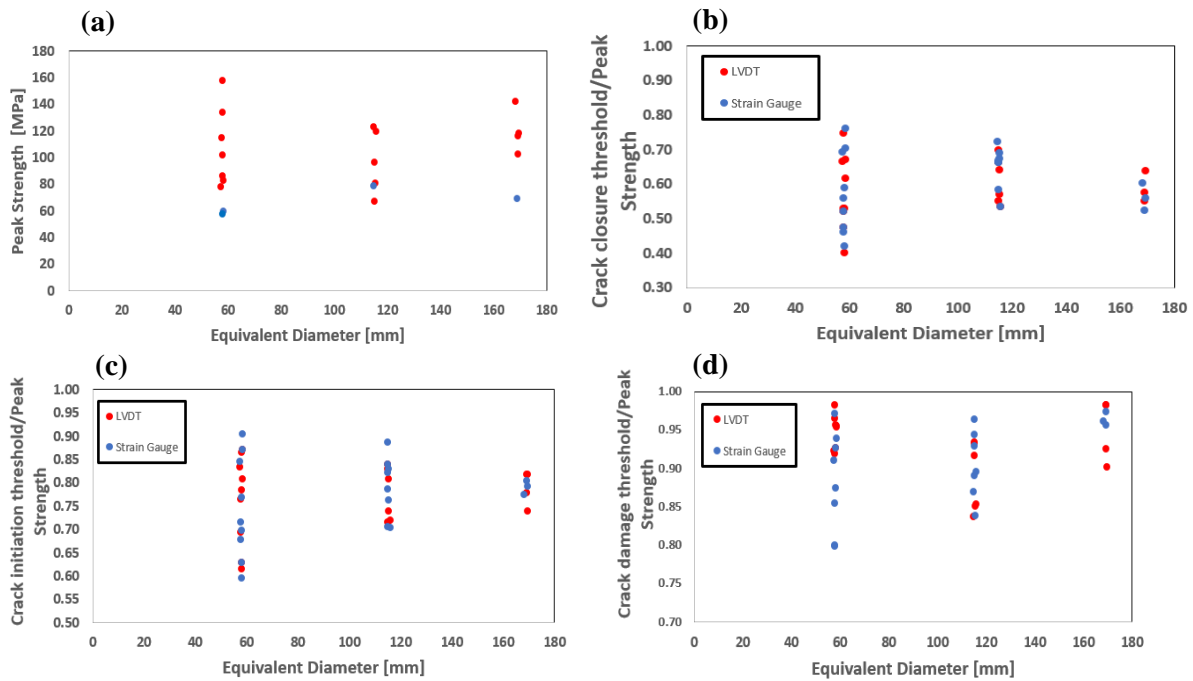

(b)

(c)

(d)

FIGURE 2.9: SUMMARY OF PARAMETERS OBTAINED AS FUNCTION OF EQUIVALENT DIAMETER: (A) PEAK STRENGTH (B) σCC AS % OF PEAK (C) σCI AS % OF PEAK, AND (D) σCD AS % OF PEAK

All diameters in Figure 2.8 and Figure 2.9 were expressed in equivalent diameter in order to normalize the results.

2.5. Conclusions

Obtaining complete stress-strain curves is highly complex in rocks with post-peak class II behavior due to the great instability of the rock against rupture. However, the methodology used based on the ISRM standard has proven to be useful in obtaining the complete curve with post-peak behavior, which allowed a high percentage of success to be achieved in the tests, especially in smaller size diameters.

The damage thresholds, peak strength, Poisson's ratio, and drop modulus did not show any indication of the scale effect. These results are conditioned by the number of samples tested, which complies with the minimum number of samples recommended by the ISRM. The number of tests is not sufficient to define a trend due to the variability observed in the mechanical properties. A possible improvement for future studies would be to increase the number of samples tested that allow statistically representative values to be obtained. In addition, the range and number of diameter sizes should be increased to include smaller diameter sizes, such as d = 25mm, and larger sizes, such as d = 200 mm. On the other hand, it is also suggested that tests should be performed with other initial conditions that may influence the results, such as the type of rock, the presence of discontinuities, or the shape effect. Only samples with no visible defects or discontinuities are included in the tests, this could be one of the reasons of peak strength did not show scale effect.

A new parameter was introduced called diametral residual stress, which refers to a constant stress value for which the sample constantly increases its diametral strain because of the propagation of the generated cracks. This parameter seems to indicate that there is a scale effect according to the results obtained, supported by visual verification of a greater fracture propagation at larger

diameters. However, this trend should be verified by increasing the number of samples tested and expanding the range of diameter sizes and other types of rock that show class II post-peak behavior. Future work could consider the use of direct strain measurement instruments, i.e. attached to the samples, that allow a more complete measurement of perimeter and height to capture the deformations that occur throughout the length and width of the sample. The measurement of only local deformations, such as those that can be obtained with strain gauges, could lead to errors in the estimation of the parameters and make it impossible to obtain post-peak parameters. Another possible improvement to this study could be the use of triaxial-test results to complement the uniaxial tests presented here, which could allow the visualization of changes in behavior and parameters at different confinements.

Finally, it is important to emphasize that this is a preliminary study to identify the potential to better understand the behavior of rock mass. Future studies that test other types of rocks, other stress conditions such as triaxial tests, and that use direct strain instruments for measuring deformation, and other initial conditions would be helpful to better understand the post-peak behavior at a laboratory scale. However, the results obtained in this study are significant as they provide additional information for the world database of rock mechanics on post-peak behavior.

2.6. Acknowledgement

3. Conclusions and Future Work

3.1. General Conclusions

The results from the set of uniaxial tests with post-peak behavior have yielded post-peak class II curves, for which the main parameters are within the expected range (80-120 MPa of UCS, 30-40 GPa Young's modulus, 0.2-0-3 Poisson's ratio and 30-40 Drop Modulus) found in the literature.

The proposed methodology has shown to be capable of obtaining complete stress-strain curves in rocks with post-peak class II behavior for the different diameters tested. Although this methodology has been developed empirically in conjunction with the suggestions of previous works, slight modifications were made that aimed to increase the speed of the test in order to reduce its duration. These modifications have not been successful, despite meeting the ISRM recommendations, because the fractures propagation in the samples were unstable (Figure 2.7). This suggests that the maximum speed that allows the complete stress-strain curve to be obtained could be closely related to some of the parameters that define post-peak behavior.

Although this study seeks to evaluate the scale effect in intact rock, the difficulty of finding intact rock samples (free of discontinuities) in diameter sizes larger than those tested in this study could be a limitation to evaluate this effect in larger sizes. This is more relevant since, although most of the samples tested in this study have been classified as intact rock, rocks that had one or more discontinuities have been tested for other authors (Arzua 2015, Turichshev & Hadjigeorgiou 2014), and although the complete curve could be obtained in those rocks, the results have been considerably different.

The results of this study have proven valuable to expand a database that has been lacking in tests on different diameters. Despite this, the direct application of these results to current uses, such as numerical modeling, is not entirely feasible; most models, such as the CWFS, consider brittle rocks only in the case that the drop modulus is 0, so the post-peak class II behavior does not fit these models well.

3.2. Recommendations and Future Work

A variety of opportunities for improvement in conducting studies can be identified to expand on the work presented here. In the first place, the deformation measurement methods must be standardized. Theoretically, both LVDTs and strain gauges must register the same deformations (because both aims to measurement the same axial and diametral strain in the same rock), and for this to occur, a mathematical adjustment (for example, a linear fit) must be made to the deformations measured with LVDT to calibrate these to strain gauge measurements. Another possible improvement would be to use circumferential extensometers, which can measure the complete deformation of the perimeter of the samples, avoiding possible deviations produced by the locally measured deformations of LVDTs and Strain Gauges.

CHAPTER 3

Furthermore, most of the results are independent of the scale. Then, to confirm that results are conclusive, a greater number of samples (five samples more, minimum according ISMR suggestions) of the same lithology should be included that complement the results obtained. In this way, the impact of factors such as geological variability or the effectiveness of the methodology could be reduced. Along this same line, another recommendation is to increase the range of diameters used in this study, both for larger and smaller diameters. This would allow trends to be evaluated in a wider range of diameters and to reaffirm what has been found in the diametral residual stress. In addition, it would allow further study to confirm that the scale effect is not present in other parameters.

This preliminary study could also be expanded with triaxial tests to measure the complete stress-strain curve; this would allow the transition from brittle to ductile to be observed. It would also provide the opportunity to apply results to constitutive models and thus to study new parameters.

Another important step is to complement the study with uniaxial tests of the same lithology, but with changes in the initial conditions, such as varying the height/diameter ratio, temperature of the tests or humidity of the rocks, the lithology and/or the presence of discontinuities, among others. A more complete set of tests would be valuable to evaluate the impact of each of these factors on post-peak behavior.

Finally, doing additional tests will allow the methodology to be consolidated as each of the changes or supplementary measurements suggested above may need to slightly or completely modify the methodology to obtain the best possible results. In this way, the proposed methodology could be improved, generalized or standardized for any type of uniaxial test under various initial conditions.

CHAPTER 4

4. Bibliography

Akinbinu, VA 2015, 'Increasing effect of metamorphism on rock properties', International Journal of Mining Science and Technology, vol. 25, no. 2, pp. 205–211.

Akinbinu, VA 2016, 'Class I and Class II Rocks: Implication of Self-sustaining Fracturing in Brittle Compression', Geotechnical and Geological Engineering, vol. 34, no. 3, pp. 877–887.

Alejano, LR, Arzúa, J, Castro-Filgueira, U & Kiuru, R 2018, 'Scale effect of intact Olkiluoto gneissic rocks through uniaxial compressive testing and geophysical measurements', POSIVA Working Report 2018-13. Available from: <http://www.posiva.fi/files/4890/WR2018-13_web.pdf>. [06-25-2020].

Alejano, LR, Arzúa, J, Estévez-Ventosa, X & Suikkanen, J 2020, 'Correcting indirect strain measurements in laboratory uniaxial compressive testing at various scales', Bulletin of Engineering Geology and the Environment, in press, DOI:10.1007/s10064-020-01853-4.

Arzua, J 2015, 'Study of the Mechanical Behavior of Intact and Jointed Rocks in Laboratory with Particular Emphasis on Dilatancy', PhD thesis, Universidad de Vigo, Vigo.

Basu, A, Mishra, D & Roychowdhury, K 2013, 'Rock failure modes under uniaxial compression, Brazilian, and point load tests', Bulletin of Engineering Geology and the Environment, vol. 72, no. 3, pp. 457-475.

Bear, J 1972, 'Dynamics of fluids in porous media', American Elsevier Publishing Company, New York

Cai, M, Kaiser, P, Tasaka, Y, Maejima, T, Morioka, H & Minami, M 2004, 'Generalized crack initiation and crack damage stress thresholds of brittle rock masses near underground excavations', International Journal of Rock Mechanics and Mining Sciences, vol. 41, no. 5, pp. 833-847.

De los Santos, C 2012, ´Revisión de ensayos geotécnicos en las principales unidades litológicas y vetillas del yacimiento el teniente', Internal CODELCO report, Unpublished.

Delonca, A & Vallejos, JA 2020, 'Incorporating scale effect into a failure criterion for predicting stress-induced overbreak around excavations', International Journal of Rock Mechanics & Mining Sciences, vol. 127, March 2020, 104213.

Eberhardt, E, Stead, D, Stimpson, B, & Read, RS 1998, 'Identifying crack initiation and propagation thresholds in brittle rock', Canadian Geotechnical Journal, vol. 35, no. 2, pp. 222–233.

Hajiabdolmajid, V, Kaiser, PK & Martin, CD 2002, 'Modelling brittle failure of rock', International Journal of Rock Mechanics & Mining Sciences, vol. 39, no. 6, pp. 731–741.

Hawkes, I & Mellor, M 1970, 'Uniaxial testing in rock mechanics laboratories', Engineering Geology, vol. 4, no. 3, pp. 179–285.

Hoek, E & Brown, ET 1980, 'Underground Excavations in Rock', Institution of Mining and Metallurgy, London.

Hudson, J, Brown, E & Fairhurst, C 1971, 'Optimizing the control of rock failure in servo-controlled laboratory tests', Rock Mechanics Felsmechanik Mecanique des Roches, vol. 3, no. 4, pp. 217–224.

Hudson, JA, Crouch, SL & Fairhurst, C 1972, 'Soft, stiff and servo-controlled testing machines: a review with reference to rock failure', Engineering Geology, vol. 6, no. 3, pp. 155–189.

Marambio, F, Pereira & Russo, A 1999, 'Estudio Propiedades Geotécnicas Proyecto Pipa Norte', Internal CODELCO report, Unpublished.

Masoumi, H, Saydam, S, & Hagan, PC 2016, 'Unified size-effect law for intact rock', International Journal of Geomechanics, vol. 16, no. 2, 04015059.

Meng, F, Zhou, H, Zhang, C, Xu, R & Lu, J 2015, 'Evaluation Methodology of Brittleness of Rock Based on Post-Peak Stress–Strain Curves', Rock Mechanics and Rock Engineering, vol. 48, no. 5, pp. 1787-1805.

Munoz, H, Taheri, A & Chanda, EK 2016, 'Pre-Peak and Post-Peak Rock Strain Characteristics During Uniaxial Compression by 3D Digital Image Correlation', Rock Mechanics and Rock Engineering, vol. 49, no. 7, pp. 2541–2554.

Peng, J, Cai, M, Rong, G, Yao, M, Jiang, Q, & Zhou, C 2017, 'Determination of confinement and plastic strain dependent post-peak strength of intact rocks', Engineering Geology, vol. 218, pp. 187–196.

Pollak, D, Vallejos JA 2018 'Consideraciones para ensayos de compresión uniaxial con medición de comportamiento postpeak y resultados preliminares', UMining: Congreso Iberoamericano en Minería Subterránea y a Cielo Abierto, Santiago, Chile.

Ramírez-Oyanguren P, & Alejano LR 2008, 'Mecánica de Rocas: Fundamentos e Ingeniería de Taludes', Red DESIR, Madrid.

Roshan, H, Masoumi, H & Regenauer-Lieb, K 2017 'Frictional behaviour of sandstone: A sample-size dependent triaxial investigation', Journal of Structural Geology, vol. 94, January 2017, pp. 154–165.

Rummel, F 1972, 'Brittle Fracture of Rocks', in L Muller (ed.), Rock Mechanics, Springer Verlag, Wien, pp. 85–94.

Schultz, R 1995, 'Limits on strength and deformation properties of jointed basaltic rock masses', Rock Mechanics and Rock Engineering, vol. 28, no. 1, pp. 1–15.

Servosis 2020, Software de control PCD2K. Available from: <https://www.servosis.com/productos/pcd2k>. [20-06-2020].

Susheng, W, Huanling, W, Weiya, X & Wei, Q 2019, 'Investigation on mechanical behavior of dacite under loading and unloading conditions', Géotechnique Letters, vol. 9, no. 2, pp. 130-135.

Turichshev, A & Hadjigeorgiou, J 2014 'Experimental and Numerical Investigations into the Strength of Intact Veined Rock', Rock Mechanics and Rock Engineering, vol. 48, no. 5, pp. 1897–1912.

CHAPTER 4

Turichshev, A & Hadjigeorgiou, J 2016, 'Triaxial compression experiments on intact veined andesite', International Journal of Rock Mechanics and Mining Sciences, vol.86, pp. 179-193.

Ulusay, R & Hudson JA 2007, 'The complete ISRM suggested methods for rock characterization, testing and monitoring: 1974–2006. Prepared by the commission on testing methods', ISRM Turkish National Group, Ankara.

Walton, G 2017, 'Scale Effects Observed in Compression Testing of Stanstead Granite Including Post-peak Strength and Dilatancy', Geotechnical and Geological Engineering, vol. 36, no. 4, pp. 1091–1111.

Walton, G 2019, 'Initial guidelines for the selection of input parameters for cohesion-weakening-friction-strengthening (CWFS) analysis of excavations in brittle rock', Tunnelling and Underground Space Technology, vol. 84, pp. 189-200.

Yoshinaka, R, Osada, M, Park, H, Sasaki, T, & Sasaki, K 2008, 'Practical determination of mechanical design parameters of intact rock considering scale effect', Engineering Geology, vol. 96, no. 3, pp. 173–186.

Zhang, H & Li, C 2018, 'Effects of Confining Stress on the Post-Peak Behaviour and Fracture Angle of Fauske Marble and Iddefjord Granite', Rock Mechanics and Rock Engineering, vol. 52, no. 5, pp. 1377-1385.

Zhao, X & Cai, M 2010, 'A mobilized dilation angle model for rocks', International Journal of Rock Mechanics and Mining Sciences, vol. 47, no. 3, pp. 368–384.

A. Complementary Material for Chapter 2

The following section covers complementary material for the implementation of the methodology and results of the article presented in Chapter 2.

A.1. Complementary Material for Methodology

A.1.1. Structural Mapping

The presence of structures or discontinuities can considerably affect the results and parameters of compression tests, and for this reason geologically and structurally identifying these discontinuities is proposed. It is possible to see in some of the prepared samples (Appendix Figure A.1) the presence of discontinuities of considerable thickness, so the proposed characterization is highly necessary to analyze the results obtained.

The proposed methodology is summarized in the following steps:

Reference lines: 4 reference lines (Black, Blue, Red and Green) are drawn on the surface of the samples vertically and separated from each other at 90º. One cm should be left on the upper and lower edges, delimiting with circumferential lines to avoid irregularities at the edge of the samples. The lines are also extended to the basal faces in order to be able to quickly identify and reassemble the sample once they are tested and fractures occur. The upper basal face is defined by the intersection of these four lines in the center of the sample, while on the lower basal face, these lines reach ½ of the radius from the outside of the sample to the inside. Finally, a photographic record of the sample is made of each vertical line drawn and both basal faces.

APPENDIX FIGURE A.1: EXAMPLE OF LINES REFERENCE LINES. LEFT, UPPER BASAL FACE. CENTER, VERTICAL REFERENCE LINES. RIGHT, BUTTON BASAL FACE

Vein marking: A transparent paper or transparent mica sheet must be cut with the same dimensions as the sample that is being mapped. This mica is superimposed around the sample and on it the

APPENDIX

reference lines of the sample are first drawn and then the discontinuities previously identified are drawn with a visual review. Subsequently, a photographic record of the mica is made, and a photographic record of the complete surface of the sample is obtained with a camera with panoramic function to compare the mica and surface photographs and verify correct performance.
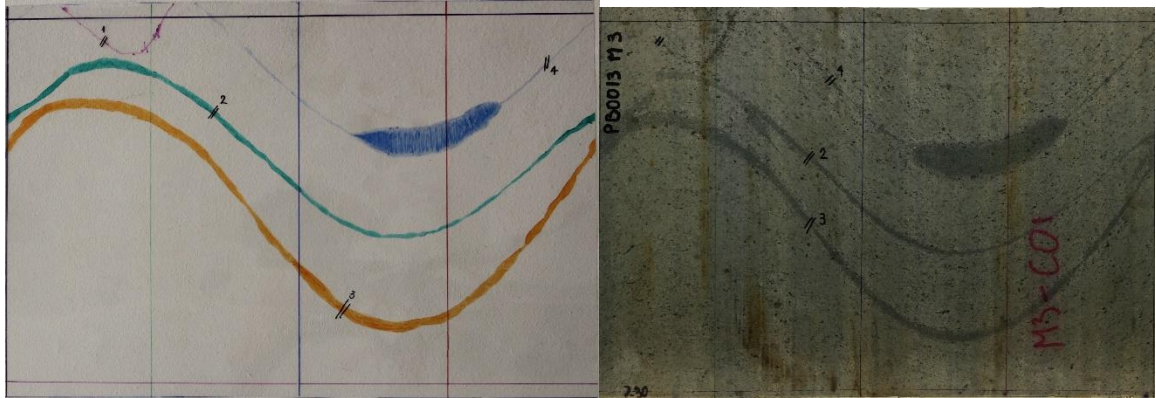
APPENDIX FIGURE A.2: EXAMPLE OF PHOTOGRAPHY RECORD OF SURFACE SAMPLE (LEFT) AND SURFACE MAPPING (RIGHT)

Description of the rock: The description of the rock should include the main minerals that make up the fundamental matrix (describing habit, microstructure, size, disposition and percentage of abundance). Other parameters must also be described, such as color, texture, percentage of fundamental mass and phenocrysts, structure and morphology. Additionally, it is advisable to make thin sections so as to obtain greater precision in data collection through microscopic analysis of fundamental mass.

APPENDIX TABLE A.1: GEOLOGICAL CHARACTERIZATION OF ROCK SPECIMENS

Description of the rock		
1. General features		
Color	Whitish green	
Texture	Porphyry	
Color index	Clear Minerals	80%
	Dark Minerals	20%
Fundamental Mass	80%	
Phenocrystal	20%	
Structure	Homogeneous	
Grain orientation	Isotropic	
Morphologies	Not observed	
2. Mineralogy		
Mineral 1	Quartz	
Crystal Habit	Massive	
Microstructure	Anhedral	
Size	Not measurable	
Appearance	Fundamental mass	
% Abundance	30% of the rock	

APPENDIX

Description of the rock		
Mineral 2	**Plagioclase**	
Crystal Habit	Massive	
Microstructure	Anhedral	
Size	Not measurable	
Appearance	Fundamental mass	
% Abundance	35% of the rock	
Mineral 3	**Feldspars**	
Crystal Habit	Massive	
Microstructure	Anhedral	
Size	Not measurable	
Appearance	Fundamental mass	
% Abundance	15% of the rock	
Mineral 4	**Biotite**	
Crystal Habit	Micaceous to Massive	
Microstructure	Subhedral to Anhedral	
Size	Fine grain (less than 2 mm)	
Appearance	Phenocrysts	
% Abundance	20% of the rock	
3. Name of the rock		
Q	37.5%	dacite
A	18.75%	
P	43.75%	

Appendix Figure A.3 shows examples of the thin sections used for the geological characterization of the samples. A total of ten thin sections were made from different initial sample pieces. There were no significant differences in the geological composition of the samples, which is why the samples are considered homogeneous.
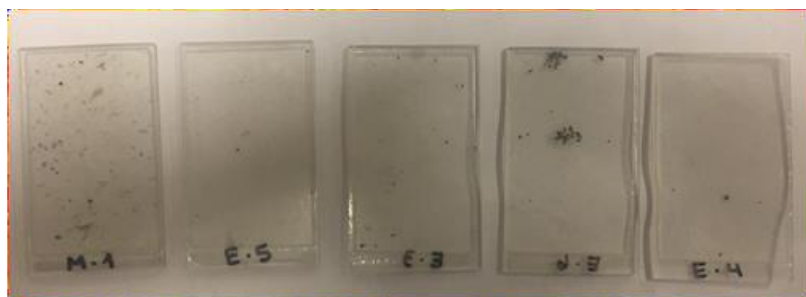
APPENDIX FIGURE A.3: THIN SECTIONS OF DACITE ROCK FOR GEOLOGICAL CHARACTERIZATION

APPENDIX

A.1.2.   Compression Test Set-up

The setup for each of the three diameter sizes tested is shown below. At this point, it is important to note that for the 50 mm diameter samples, an aluminum ring was used to support the LVDTs because the magnetic bases are too high to be placed inside the equipment.
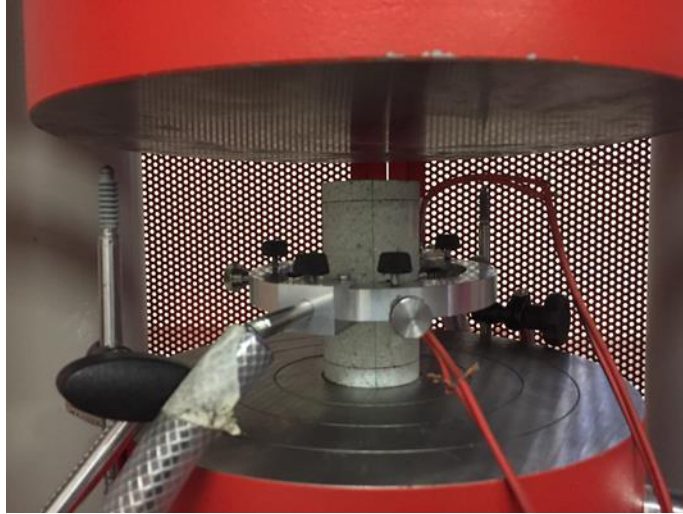
APPENDIX FIGURE A.4: SET-UP FOR 50 MM DIAMETER SPECIMENS

APPENDIX FIGURE A.5: SET-UP FOR 98 MM DIAMETER SPECIMENS

APPENDIX

APPENDIX FIGURE A.6: SET-UP FOR 143 MM DIAMETER SPECIMENS

A.2.   Complementary Material of Results

A.2.1.   Complete Stress-strain Curves

The methodology proposed for carrying out simple compression tests to control diametral deformation was used in the 30 available samples. However, it was not possible to obtain the post-peak behavior in all the samples tested. The tests had different success rates with different sizes. For the 50 mm diameter samples, 9 out of 10 tests were successful in obtaining the stress-strain curve (Appendix Figure A.7). On the other hand, for the 98 mm diameter samples, 7 out of 10 proved to be successful tests (Appendix Figure A.9), while for the 143 mm diameter samples, only 5 out of 10 were successful tests (Appendix Figure A.11).

APPENDIX

STRESS-STRAIN CURVES – 50 MM DIAMETER SPECIMENS
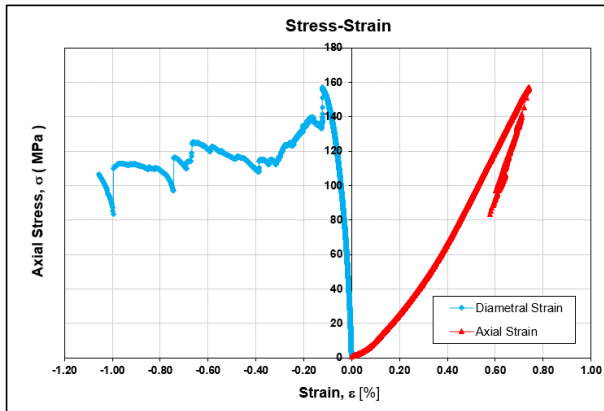
Sample M4A

Sample M5D
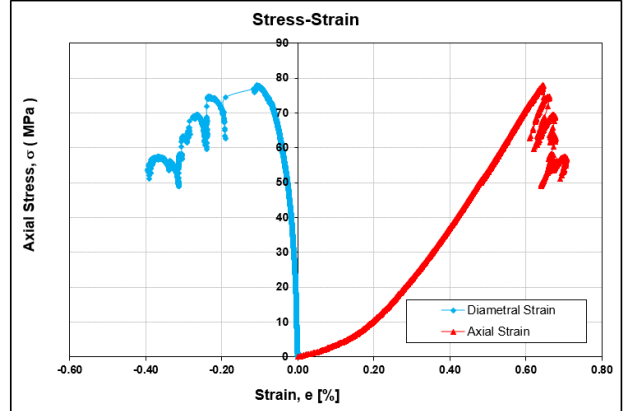
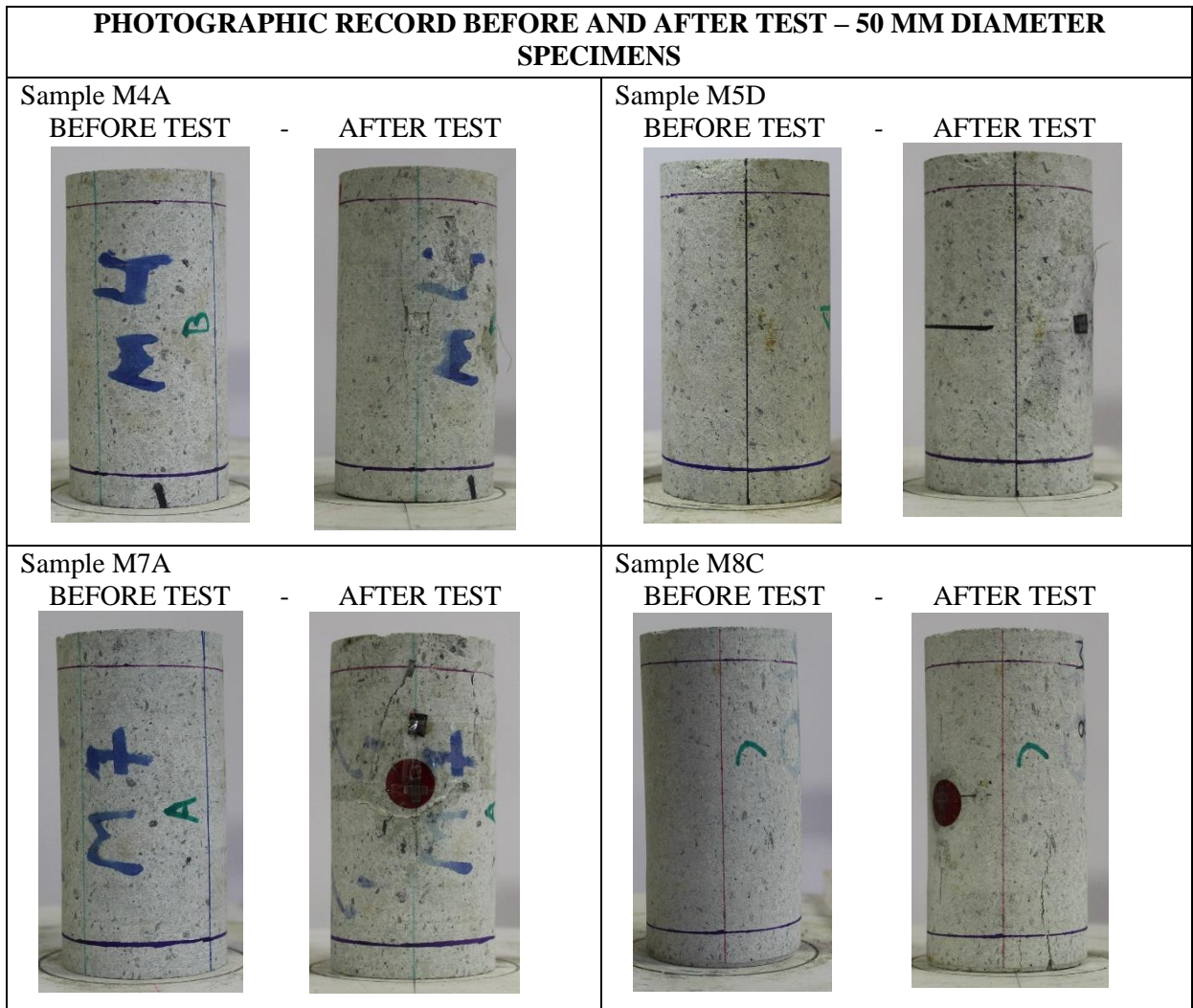
Sample M7A
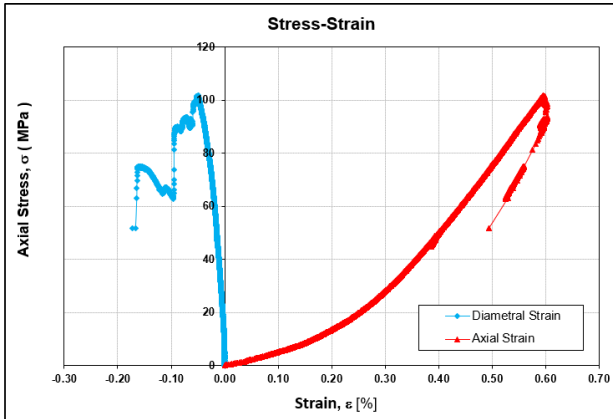
Sample M8C
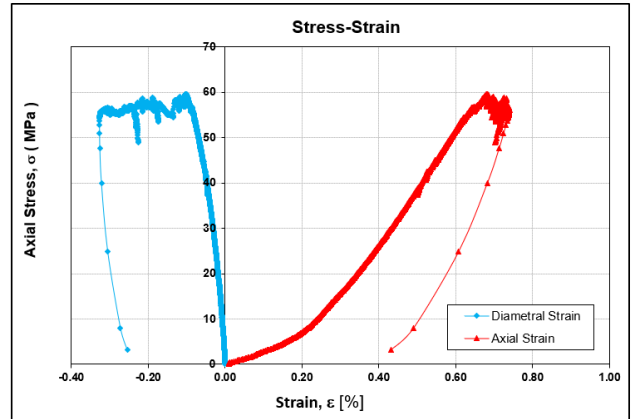
Sample M8D
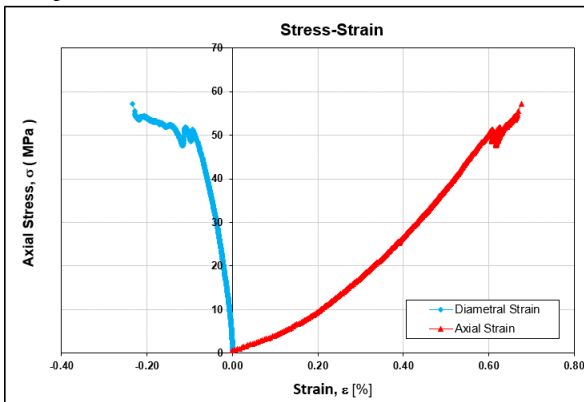
Sample M9C
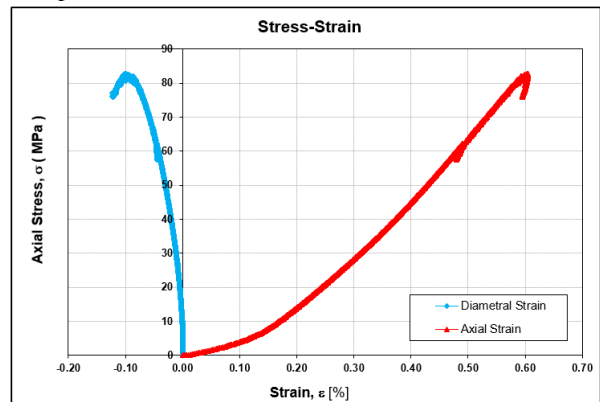
APPENDIX FIGURE A.7: RESULTING STRESS-STRAIN CURVES FOR 50 MM DIAMETER SPECIMENS

APPENDIX

STRESS-STRAIN CURVES – 50 MM DIAMETER SPECIMENS
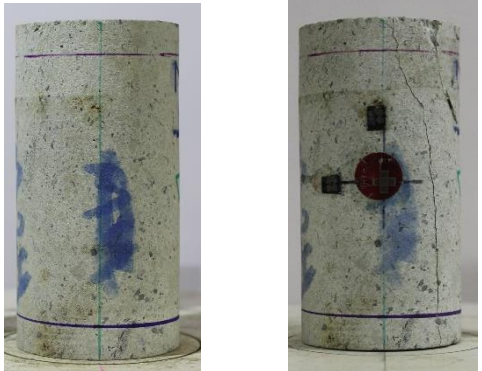
Sample M14D
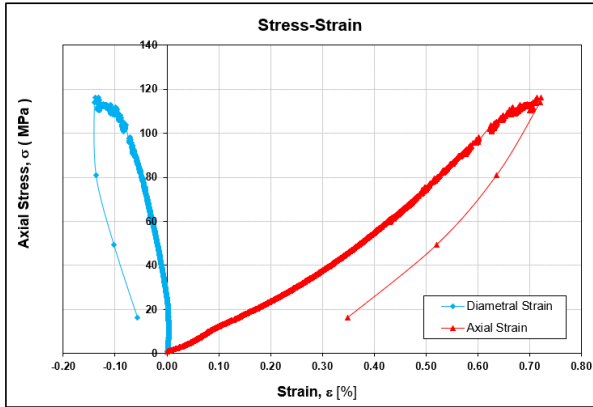
Sample M24D
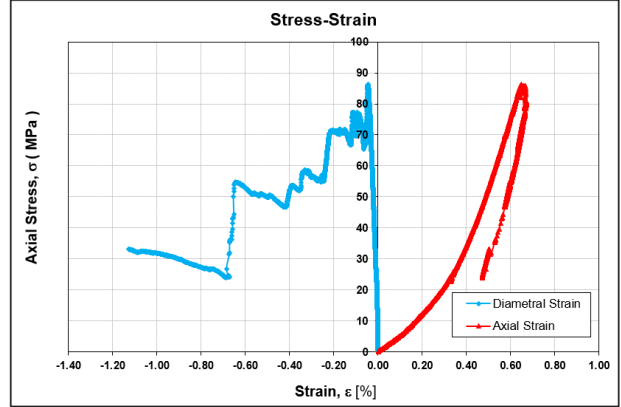
Sample M25A
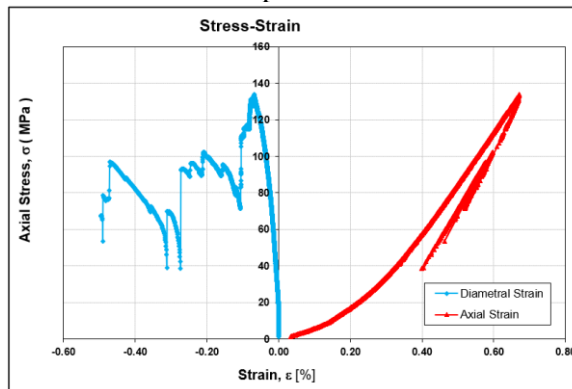
APPENDIX FIGURE A.8: RESULTING STRESS-STRAIN CURVES FOR 50 MM DIAMETER SPECIMENS (CONTINUED)

STRESS-STRAIN CURVES – 98 MM DIAMETER SPECIMENS
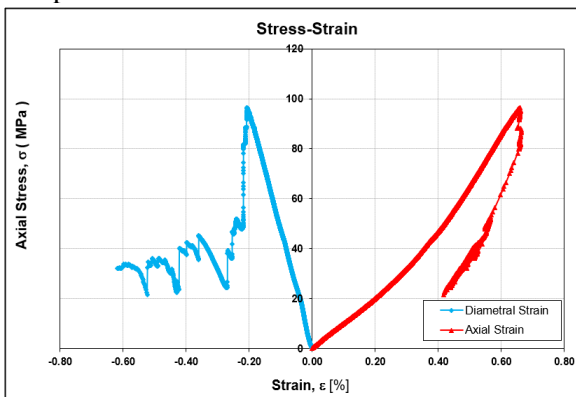
Sample M02

Sample M03
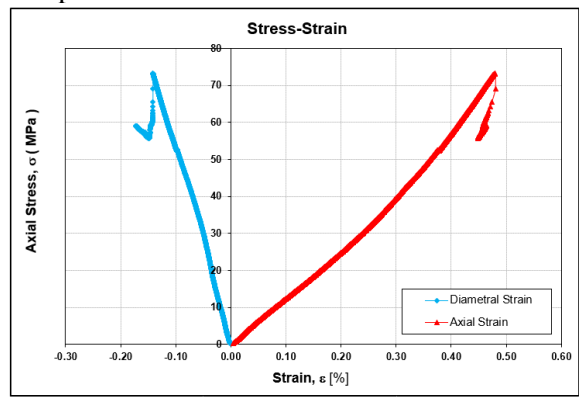
APPENDIX FIGURE A.9: RESULTING STRESS-STRAIN CURVES FOR 98 MM DIAMETER SPECIMENS

APPENDIX

STRESS-STRAIN CURVES – 98 MM DIAMETER SPECIMENS

Sample M06
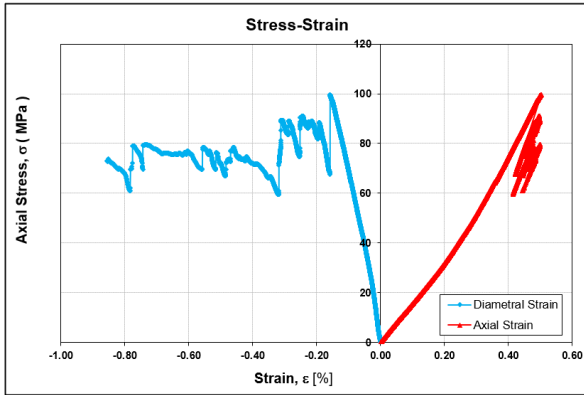
Sample M08
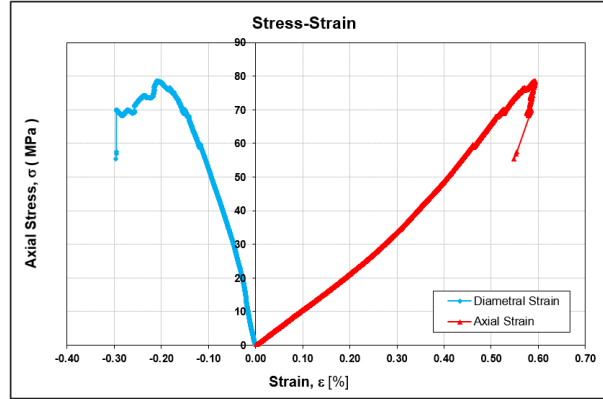
Sample M11
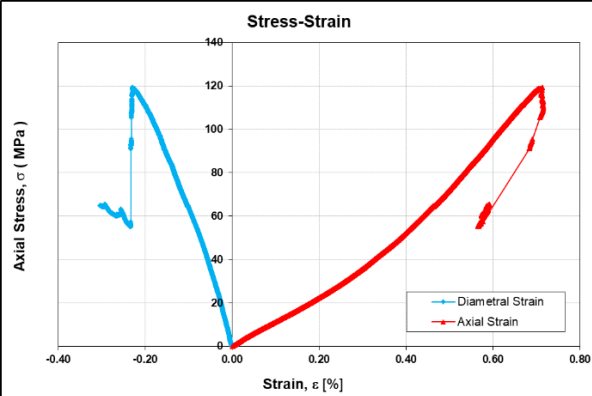
Sample M15
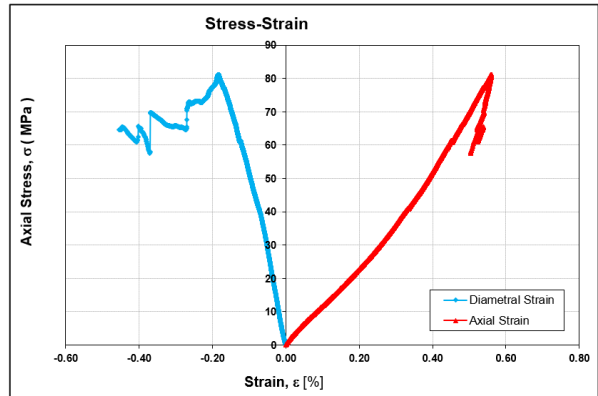
Sample M18

Sample M22

APPENDIX

STRESS-STRAIN CURVES – 143 MM DIAMETER SPECIMENS
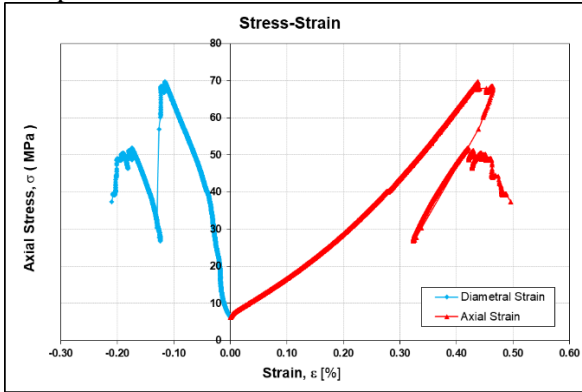
Sample M08

Sample M12
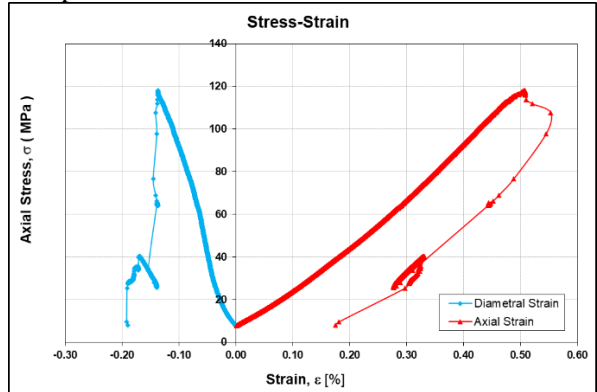
Sample M22
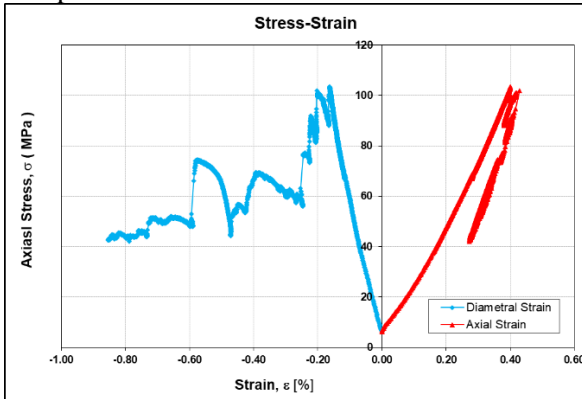
Sample M24
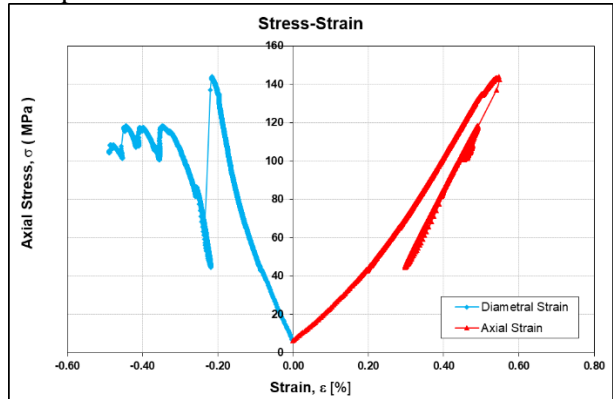
Sample M26
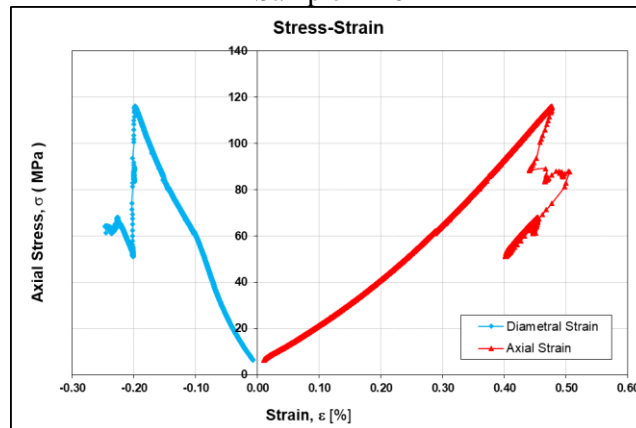
APPENDIX FIGURE A.11: RESULTING STRESS-STRAIN CURVES FOR 143 MM DIAMETER SPECIMENS
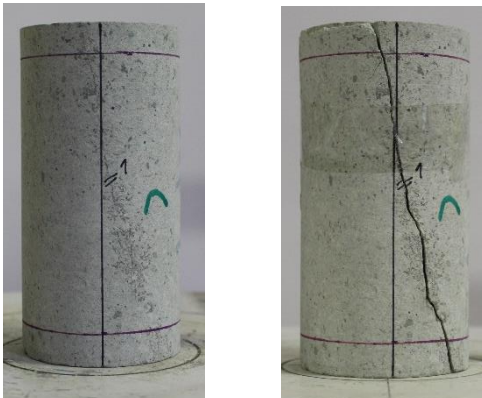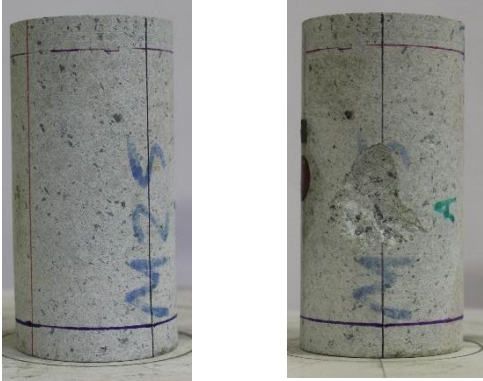
APPENDIX

A.2.2.   Photographic Record and Failure Mode

For each of the successful tests presented above, the photographic record before and after the tests allowed the failure mode of each one to be identified.
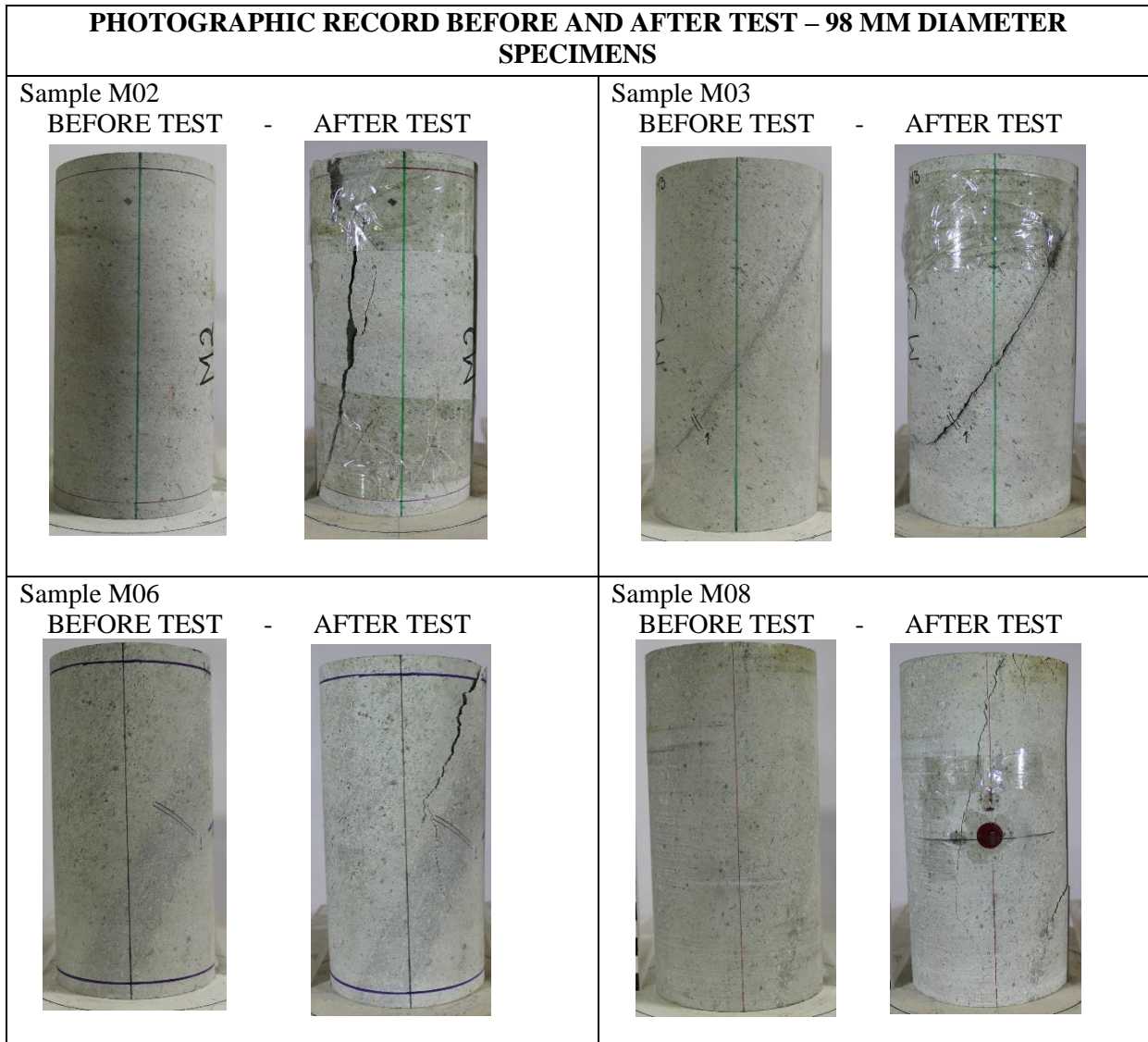
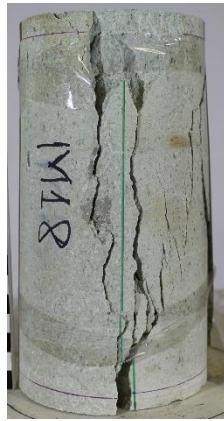| PHOTOGRAPHIC RECORD BEFORE AND AFTER TEST – 50 MM DIAMETER SPECIMENS	
Sample M4A BEFORE TEST - AFTER TEST 	Sample M5D BEFORE TEST - AFTER TEST
Sample M7A BEFORE TEST - AFTER TEST 	Sample M8C BEFORE TEST - AFTER TEST

APPENDIX FIGURE A.12: PHOTOGRAPHIC RECORD BEFORE AND AFTER TEST FOR 50 MM DIAMETER SPECIMENS

APPENDIX

PHOTOGRAPHIC RECORD BEFORE AND AFTER TEST – 50 MM DIAMETER SPECIMENS

Sample M8D
  BEFORE TEST   -   AFTER TEST

Sample M9C
  BEFORE TEST   -   AFTER TEST

Sample M14D
  BEFORE TEST   -   AFTER TEST

Sample M24D
  BEFORE TEST   -   AFTER TEST

Sample M25A
BEFORE TEST   -   AFTER TEST

APPENDIX FIGURE A.13: PHOTOGRAPHIC RECORD BEFORE AND AFTER TEST FOR 50 MM DIAMETER SPECIMENS (CONTINUED)

APPENDIX

PHOTOGRAPHIC RECORD BEFORE AND AFTER TEST – 98 MM DIAMETER SPECIMENS

Sample M02
BEFORE TEST   -   AFTER TEST

Sample M03
BEFORE TEST   -   AFTER TEST

Sample M06
BEFORE TEST   -   AFTER TEST

Sample M08
BEFORE TEST   -   AFTER TEST

APPENDIX FIGURE A.14: PHOTOGRAPHIC RECORD BEFORE AND AFTER TEST FOR 98 MM DIAMETER SPECIMENS

APPENDIX

PHOTOGRAPHIC RECORD BEFORE AND AFTER TEST – 98 MM DIAMETER SPECIMENS

Sample M11

BEFORE TEST   -   AFTER TEST

Sample M15

BEFORE TEST   -   AFTER TEST

Sample M18

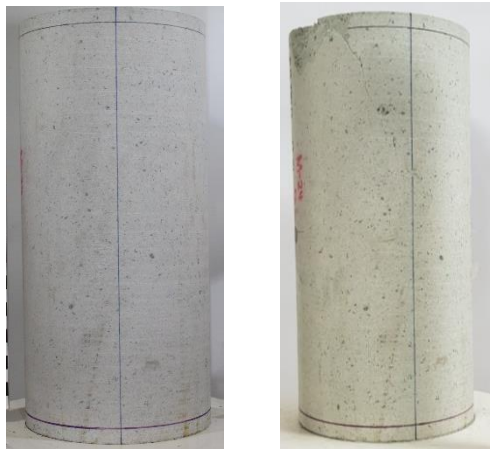BEFORE TEST   -   AFTER TEST

Sample M22

BEFORE TEST   -   AFTER TEST

APPENDIX FIGURE A.15: PHOTOGRAPHIC RECORD BEFORE AND AFTER TEST FOR 98 MM DIAMETER SPECIMENS (CONTINUED)
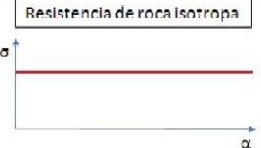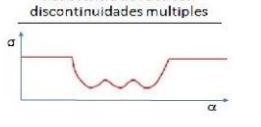
APPENDIX
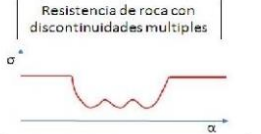
PHOTOGRAPHIC RECORD BEFORE AND AFTER TEST – 98 MM DIAMETER SPECIMENS

Sample M08

BEFORE TEST   -   AFTER TEST

Sample M12

BEFORE TEST   -   AFTER TEST

Sample M22

BEFORE TEST   -   AFTER TEST

Sample M24

BEFORE TEST   -   AFTER TEST

Sample M26

BEFORE TEST   -   AFTER TEST

APPENDIX FIGURE A.16: PHOTOGRAPHIC RECORD BEFORE AND AFTER TEST FOR 143 MM DIAMETER SPECIMENS

APPENDIX

Regarding the failure modes, these are classified according to Marambio et al. (1999), as shown in Appendix Table A.1. In addition, a classification of failure modes by Basu et al. (2013) in Appendix Figure A.17, which focuses mainly on intact rock failure modes in uniaxial compression tests, which allows a better characterization of type A failure modes.

APPENDIX TABLE A.3: DESCRIPTION OF DIFFERENT FAILURE MODES (MARAMBIO ET AL. 1999)

Tipo	Características		Esquema	Curva de resistencia
Tipo A	**Ruptura por roca.** Se caracteriza por definir una o más superficies irregulares que atraviesan indistintamente tanto la roca como las vetillas, sin desarrollarse a través de estas últimas, es decir no existe efecto de las vetillas en esta ruptura. Como resultado se genera una probeta fracturada en múltiples fragmentos.			Resistencia de roca isotropa
Tipo B	**Ruptura Mixta.** La ruptura se propagada simultáneamente a través de la roca y la vetilla, se reconocen dos subtipos.	**B1: Superficie única mixta:** Con solo una superficie de ruptura, la que se propaga por la roca y en parte por la vetilla, generando dos fragmentos en la probeta. **B2: Superficie múltiples mixta:** desarrolla varios superficie de ruptura, que se propagan por la roca y las vetillas, rompiendo la probeta en varios fragmentos.	B1 B2	Resistencia de roca con discontinuidades multiples
Tipo C	**Ruptura por varias vetillas** La ruptura se propaga por más de una vetilla en forma simultánea, generando varios trozos de roca			Resistencia de roca con discontinuidades multiples
Tipo D	**Ruptura por una vetilla.** Probeta falla por una sola vetilla. Se reconocen dos subtipos.	**D1: Superficie Única:** Se genera solo una superficie de ruptura desarrollada por una vetilla dividiendo la probeta en dos trozos. **D2: Superficie múltiple:** Presenta varias superficies de rupturas, uno principal desarrollado a través de una vetilla y los demás planos se ubican a un solo lados de la vetilla fallada interrumpiéndose contra ella.	D1 D2	Resistencia de roca anisotropa
Tipo E	Agrupan las rupturas anómalas, causada por defecto del ensayo y/o defecto en la preparación de la probeta. Puede deberse también a problemas intrínsecos del material ensayado por lo tanto los valores de resistencia obtenidos serán anómalos.		-	-
Simbología	— Vetillas — Curva de resistencia	σ: Resistencia axial α: Angulo entre la discontinuidad y el eje de longitudinal de la probeta.		Probeta (Roca intacta)
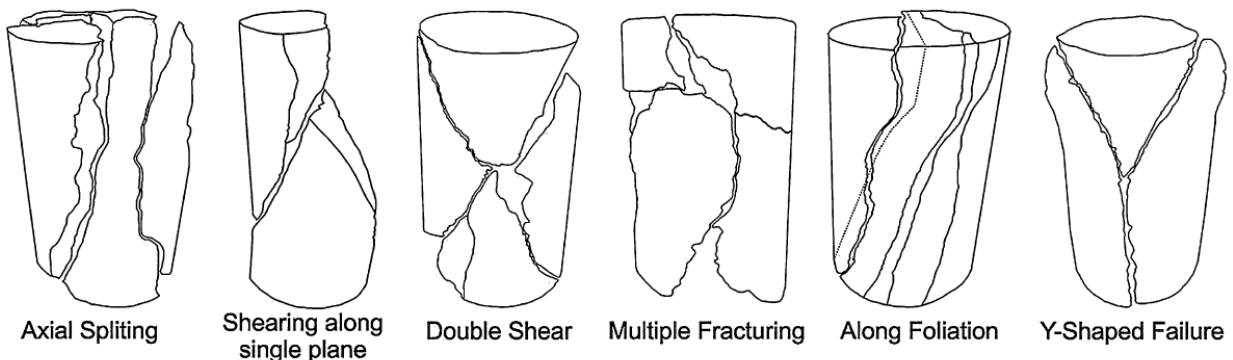
APPENDIX FIGURE A.17: SCHEMATIC REPRESENTATION OF DIFFERENT FAILURE MODES UNDER UNIAXIAL COMPRESSION (BASU ET AL. 2013)

Axial Spliting — Shearing along single plane — Double Shear — Multiple Fracturing — Along Foliation — Y-Shaped Failure

The failure modes observed in the uniaxial compression tests carried out in this study are summarized by size (Appendix Table A.4). Only the failure mode type A (Marambio et al. 1999) was considered in Chapter 2.

APPENDIX

APPENDIX TABLE A.4: FAILURE MODES OBTAINED EACH TEST ACCORDING MARAMBIO ET AL (1999) AND BASU ET AL. (2013)

Failure mode - 50 mm diameter samples		
Sample	Marambio Failure Mode	Basu Failure Mode
M4A	A	Axial Splitting
M5D	A	Axial Splitting
M7A	A	Axial Splitting
M8C	A	Axial Splitting
M8D	A	Axial Splitting
M9C	D1	Shearing along single plane
M14D	A	Axial Splitting
M24D	A	Axial Splitting
M25A	A	Axial Splitting
Failure mode - 98 mm diameter samples		
Sample	Marambio Failure Mode	Basu Failure Mode
M02	A	Axial Splitting
M03	D1	Shearing along single plane
M06	A	Axial Splitting
M08	A	Axial Splitting
M11	A	Axial Splitting
M15	A	Axial Splitting
M18	A	Axial Splitting
M22	A	Axial Splitting
Failure mode - 143 mm diameter samples		
Sample	Marambio Failure Mode	Basu Failure Mode
M08	A	Axial Splitting
M12	A	Axial Splitting
M22	B1	Double Shear
M24	A	Axial Splitting
M26	A	Axial Splitting

A.2.3.   Pre- and Post-peak Parameters

Applying the methodology for the calculation of the pre-peak parameters and the same techniques adjusted for the post-peak parameters, the detail of the results obtained for the values of the calculated parameters is presented (Appendix Table A.5). Again, it should be noted that the post-peak parameters are only calculated from the deformations measured with the LVDTs.
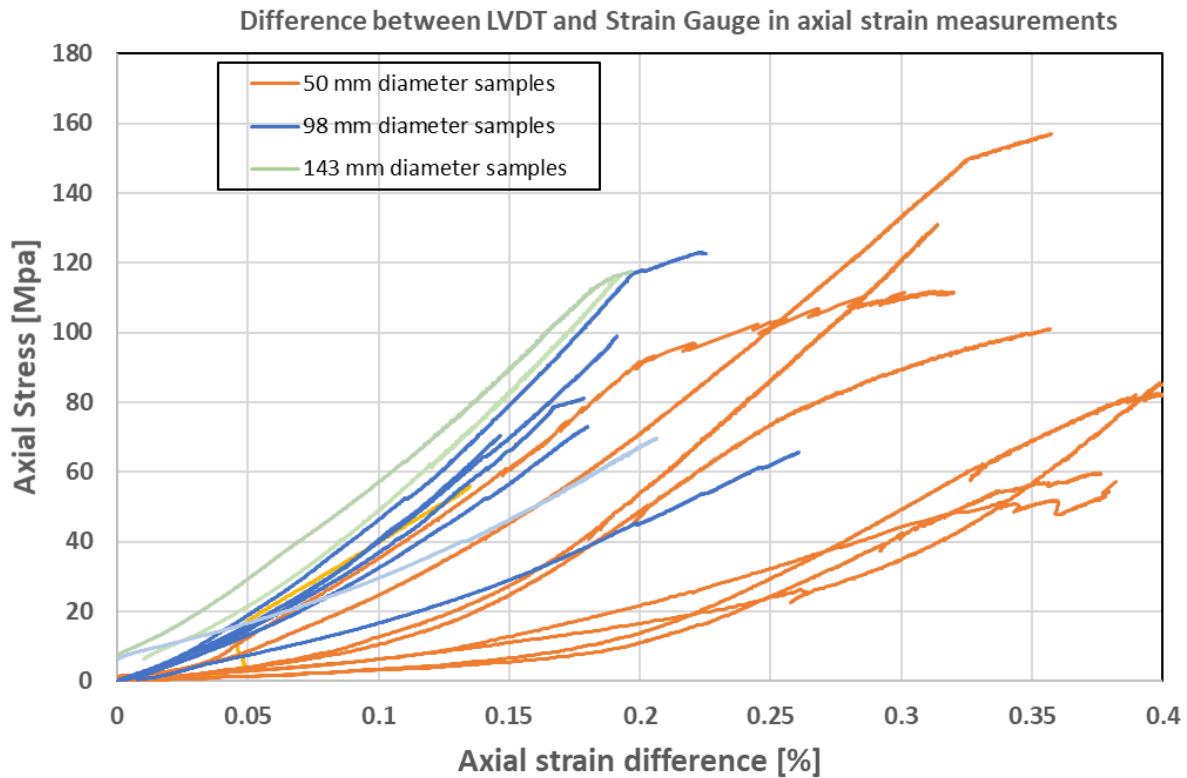
APPENDIX

| Specimen Code	Peak strength (MPa)	Equivalent diameter (mm)	LVDT E (GPa)	LVDT Poisson	Strain Gauge E (GPa)	Strain Gauge Poisson	Drop modulus (GPa)	Residual strength (MPa)
M4A	157.7	57.8	25.4	0.15	48.5	0.29	41.2	115
M5D	78.0	57.3	20.1	0.21	27.0	0.30	-	-
M7A	101.7	57.8	28.8	0.12	51.1	0.14	40.3	75
M8C	59.6	58.3	21.5	0.24	25.5	0.13	31.0	56
M8D	57.2	58.0	11.0	0.17	20.6	0.24	-	-
M9C	82.8	58.3	19.7	0.24	47.1	0.19	61.2	72
M14D	115.0	57.6	24.7	0.20	37.5	0.19	28.4	-
M24D	86.5	57.6	19.1	0.11	34.6	0.21	25.1	33
M25A	133.7	58.0	31.5	0.16	52.6	0.28	32.2	92
M02	96.4	115.2	20.2	0.31	29.4	0.35	27.4	33
M03	73.3	114.7	21.4	0.38	33.1	0.19	42.3	59
M06	99.6	115.0	25.3	0.37	41.8	0.23	49.7	76
M15	81.1	115.3	20.0	0.39	28.8	0.34	42.7	65
M18	67.4	115.0	28.3	0.39	27.4	0.16	41.3	6
M22	123.1	114.8	26.8	0.43	39.4	0.27	31.3	75
M08	78.5	114.9	18.9	0.40	29.6	0.28	45.2	70
M11	119.5	115.9	23.2	0.39	36.5	0.20	34.7	64
M22	102.6	169.2	24.0	0.35	40.1	0.23	36.8	44
M24	142.0	168.2	29.8	0.40	38.9	0.29	36.2	106
M26	116.1	169.1	29.2	0.41	43.1	0.28	33.4	63
M08	69.7	169.1	18.4	0.38	31.5	0.26	21.2	38
M12	118.1	169.4	27.9	0.32	42.3	0.28	26.2	32

APPENDIX

A.2.4. Differences in Measurements between LVDT and Strain Gauge

The previous results showed significant differences between the parameters obtained with the measurements made with the LVDTs and those made with the Strain Gauges (calculated as LVDTs strain values minus Strain Gauge strain values), which is why it was considered pertinent to make a graph that shows these differences for each test, both in axial deformation (Appendix Figure A.18) and in diametral deformation (Appendix Figure A.19). From these figures it can be deduced that there will be a significant linear correlation between the axial and diametral strain values of the samples, and consequently a correlation between their elastic parameters.

APPENDIX FIGURE A.18: DIFFERENCES BETWEEN LVDTS AND STRAIN GAUGES FOR AXIAL STRAIN MEASUREMENTS

APPENDIX

Difference between LVDT and Strain Gauge in diametral strain measurements
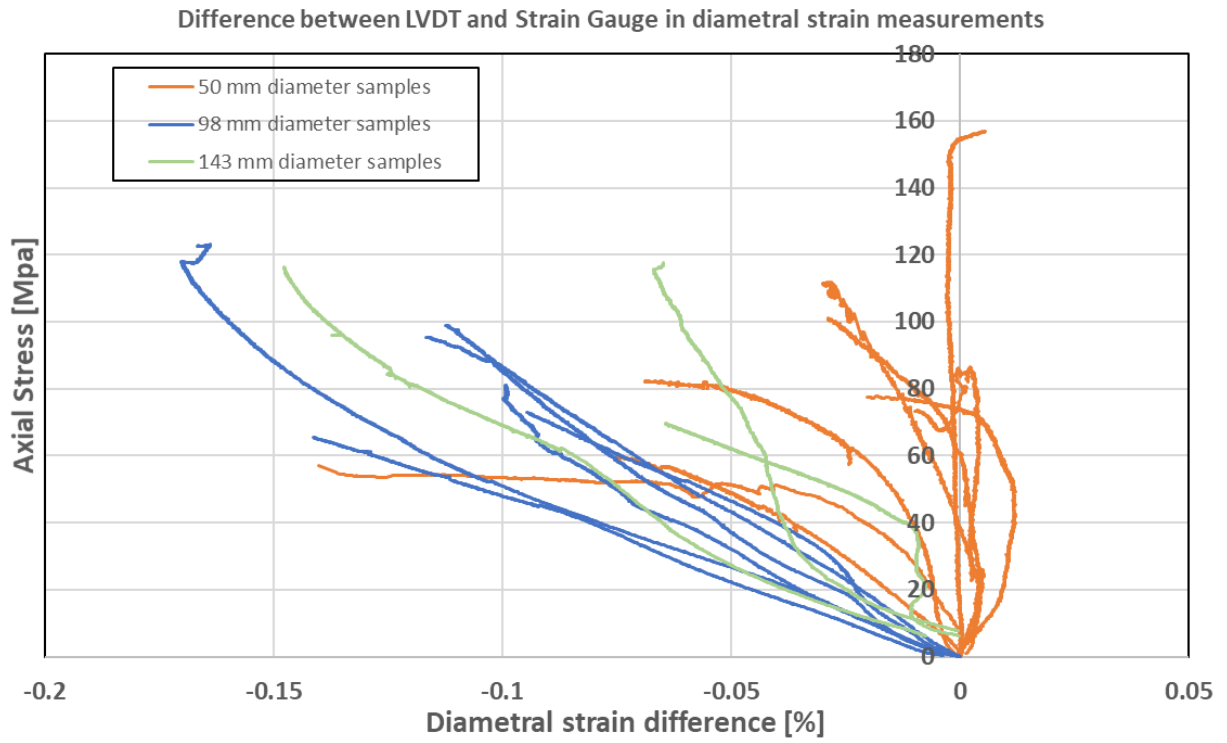
APPENDIX FIGURE A.19: DIFFERENCES BETWEEN LVDTS AND STRAIN GAUGES FOR DIAMETRAL STRAIN MEASUREMENTS